SJG
Scottish Journal of Geology

Research article

https://doi.org/10.1144/sjg2022-005 | Vol. 58 | 2022 | sjg2022-005

Investigation of coastal environmental change at Ruddons Point, Fife, SE Scotland

Sarah Louise Boyd[1,2*], Tim C. Kinnaird[1], Aayush Srivastava[1], John E. Whittaker[3] and C. Richard Bates[1]

[1] School of Earth and Environmental Sciences, University of St Andrews, Bute Building, Queen's Terrace, St Andrews KY16 9TS, Scotland, UK
[2] School of History, University of St Andrews, St Katharine's Lodge, The Scores, St Andrews KY16 9BA, Scotland, UK
[3] The Natural History Museum, Cromwell Road, London SW7 5BD, UK
SLB, 0000-0003-0386-3576; TCK, 0000-0001-6530-314X; AS, 0000-0003-2279-0843; CRB, 0000-0001-9147-7151
*Correspondence: slb78@st-andrews.ac.uk

Abstract: Ruddons Point, on the Firth of Forth coastline, Scotland, is a laterally extensive terrace of glacial and marine sediment deposits raised above current sea-level, situated near to Kincraig Point, a key site that records a series of stepped erosional platforms carved into the local bedrock, interpreted as post Last Glacial Maximum palaeoshorelines. The deposits at Ruddons Point continue inland, with exposures of the raised sands and gravels cut by the local river, the Cocklemill Burn. The site provides an opportunity to examine the depositional history through the Late Devensian and Holocene. Geophysical survey aided in interpreting characteristics of subsurface sediments such as the transition between the younger saltmarsh sediments and older underlying sands and clays below, which slope in a northerly direction. A chronology obtained through optically stimulated luminescence (OSL) dating spans from *c.* 29 ka for sands and clays at an elevation of −0.66 mOD to surface windblown sands at <300 years, at an elevation of 8.45 mOD. A basal peat, dated by radiocarbon dating to the early Holocene at *c.* 9.2 ka, formed prior to the Main Postglacial Transgression. Dating of inland raised marine deposits along the Cocklemill Burn records dates ranging from *c.* 8.9 to *c.* 4.3 ka. The raised marine deposits of Ruddons Point range from *c.* 8.1 to *c.* 2.9 ka, deposited unconformably on glacial tills and clays. This multidisciplinary field study builds depositional scenarios utilizing two dating methods, spanning the last *c.* 29 ka, to better understand coastal evolution for a region which has experienced complex relative sea-level variations.

Supplementary material: Supplementary data related to this research article is available at https://doi.org/10.6084/m9.figshare.c.6080999

Thematic collection: This article is part of the Early Career Research collection available at: https://www.lyellcollection.org/topic/collections/early-career-research

Received 21 February 2022; **revised** 24 June 2022; **accepted** 30 June 2022

Investigating our coastal landscape, and the changing environment and sedimentary depositional processes that have shaped it, is crucial to advance our understanding of climatic, crustal and sea-level responses to large-scale deglaciation. Raised deposits that are now elevated above present sea-level are common features of the Fife landscape (Sissons *et al.* 1966; Sissons 1967) and, as such, have long been of interest in reconstructing the post-glacial landscape history of eastern Scotland. However, the Fife area has few dated palaeoshorelines, so, as presently constrained, the timing of environmental changes in this area of Scotland is poorly understood. To rectify this, the Ruddons Point site in the east of Scotland [BNG NO458008] was selected for further study as it displays extensive exposures of raised deposits composed of sands, gravels and shell lags. The deposits are cut in many sections by a small river, the Cocklemill Burn, which meanders broadly west–east through the field area. The site is also of interest as glacial till and clays are exposed at the coast and provide an opportunity to investigate the timing of pre- and post-glacial sedimentation, also not clearly understood in this region.

This study expands upon previous work at this field site (Overshott 2004; Tooley and Smith 2005) by describing two separate raised deposit sections *c.* 0.5 km apart, as well as a series of cores taken through the underlying peats, sand and clays below current sea-level. The study employs initial optically stimulated luminescence (OSL) screening methods, using a portable OSL reader and simple laboratory-based quartz profiling (e.g. Kinnaird *et al.* 2017), before undertaking full OSL dating using a SAR protocol (cf. Murray and Wintle 2000). Additional radiocarbon dating was carried out at key horizons and the two approaches and results are discussed in the context of the different depositional environments across the site. This paper describes the various sediments and the relationships between them across the field site and outlines the screening methods and dating techniques used to build a chronology and interpret the environmental change since the last glacial period.

Regional setting

The Last Glacial Maximum (LGM) globally is considered to have occurred at *c.* 26 ka BP; however, the British–Irish Ice Sheet (BIIS) is thought to have developed from as early as 35–32 ka BP and reached its maximum at 27 ka BP (e.g. Chiverrell and Thomas 2010; Ballantyne and Small 2018;

Merritt *et al.* 2019). It is generally agreed that the limits of this ice sheet extended across all of mainland Scotland with deglaciation beginning after *c.* 26 ka, with the east coast becoming ice free between 21 and 16 ka, although the exact timing of ice retreat in the east of Scotland has long been debated (Peacock 2003; McCabe *et al.* 2007). Models of ice extent of the BIIS (Bradley *et al.* 2011; Kuchar *et al.* 2012) suggest that eastern Fife may have been covered by ice for in excess of 10 ka during the LGM. The pattern of movements of the BIIS in the North Sea and the final retreat of the ice sheet is thought to be highly dynamic and complex, being influenced strongly by ice streams such as the Firth of Forth ice stream which is thought to have fed the North Sea Lobe of the BIIS (Roberts *et al.* 2018; Roberts *et al.* 2019; Evans *et al.* 2021). Recent dating of offshore sediments suggests that final ice retreat into the Firth of Forth occurred by 15.8 ka (Evans *et al.* 2021). The Younger Dryas Stadial (also referred to in Britain as the Loch Lomond Stadial, LLS) was a subsequent period of cooling between 12.9 and 11.7 ka BP (Bickerdike *et al.* 2016); however, the ice sheets which centred over the western highlands are not thought to have extended as far east as Fife (Bickerdike *et al.* 2016; Ballantyne *et al.* 2021).

The early Holocene was a time of relative sea-level fall along the east coast of Scotland and previously marine and estuarine areas developed into peatlands. These buried marine sediment horizons have been referred to as 'Buried Beaches' and a Main and a Low buried beach have been distinguished, radiocarbon dated to 9.8–9.4 ka BP and 8.8–8.5 ka BP, respectively (Sissons *et al.* 1966; Smith *et al.* 2002). In the Middle Holocene the pattern of relative sea-level (RSL) fall in Scotland due to isostatic uplift was outpaced by eustatic sea-level rise, attributed to the final melting of the Laurentide ice sheet (Milne *et al.* 2006; Rennie and Hansom 2011). This rise is recorded across Scotland and is termed the Main Postglacial Transgression (Sissons 1974). The resulting estuarine deposits that built up over underlying terrestrial peat in this region are referred to as carse clay. The Storegga Slide, an underwater landslide off the coast of Norway, is thought to have occurred during the Main Postglacial Transgression, recently dated in the Montrose Basin, Angus, to 8.1 ka (Bateman *et al.* 2021). This significant landslide caused a tsunami event, which resulted in abrupt flooding along coastlines of Norway, Denmark, Greenland and the northern and eastern coastlines of Scotland and England (Kim *et al.* 2019). These deposits, also referred to as tsunamiite deposits, were first identified and linked to the Storegga Slide by Dawson *et al.* (1988) and evidence of the event has been identified in numerous locations around the Shetland Islands coastline, as well as the northern and eastern coastline of mainland Scotland and northeastern England (Costa *et al.* 2021). The Main Postglacial Transgression and steady sea-level rise culminated in the Main Postglacial Shoreline, which has been dated to 6.2–7.8 ka cal BP (Smith *et al.* 2019). Younger Holocene shorelines have also been identified around the Scottish coastline: the Blairdrummond Shoreline (*c.* 3.6–5.8 ka cal BP, Smith *et al.* 2019) and the Wigtown Shoreline (*c.* 1.2–3.2 ka cal BP, Smith *et al.* 2019). Figure 1 displays the closest modelled RSL curves to the field site in SE Fife, centred on the Forth Valley and Tay Valley regions (Shennan *et al.* 2018).

Study area

The field study location centres on Ruddons Point, situated in south Fife, on the northern coastline of the Firth of Forth (Fig. 2). The Ruddons Point promontory separates the beaches of Shell Bay to the south and Largo Bay to the north. The terrace lies *c.* 1 km to the NW of Kincraig Point terraces which are themselves a key type example of eroded shorelines where four clear platforms are cut into the local, igneous bedrock (Fig. 3). Previous researchers (Cullingford and Smith 1966; Smith *et al.* 1969; Jardine 1982) have commented on the potential age and correlation of the Kincraig Point erosional terraces as being related to the Main Perth Shoreline, a shoreline thought to have been formed during the Perth Re-advance *c.* 17.5–14.5 ka (McCabe *et al.* 2007), and Late Glacial Shorelines; however, no absolute dating has been undertaken to confirm this. The Ruddons Point sand, shell and gravel deposits sit above a unit of glacial till and underlying clays which themselves have been deposited unconformably on Carboniferous–Permian age basaltic intrusive sequences (Chapman 1976). These intrusives sit within the wider bedrock geology of the study site, which is composed of Carboniferous limestone and coal

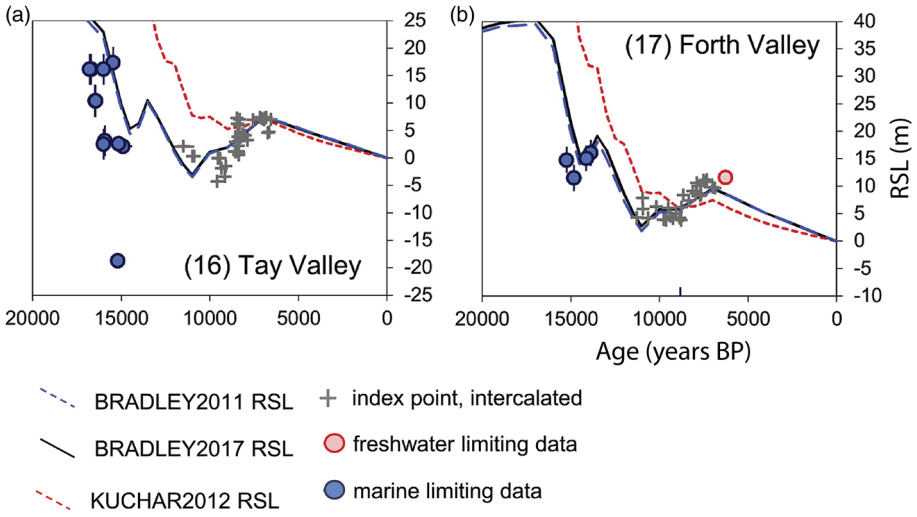

Fig. 1 Age–elevation graphs of modelled relative sea-level (RSL) over the last 20 ka for (**a**) the Tay Valley region and (**b**) the Forth Valley region (plots 16 and 17 from Shennan *et al.* 2018, fig. 7). The plots display RSL models from Bradley *et al.* (2011), Kuchar *et al.* (2012) and a new model, BRADLEY2017, along with index points and freshwater and marine limiting data points for each region.

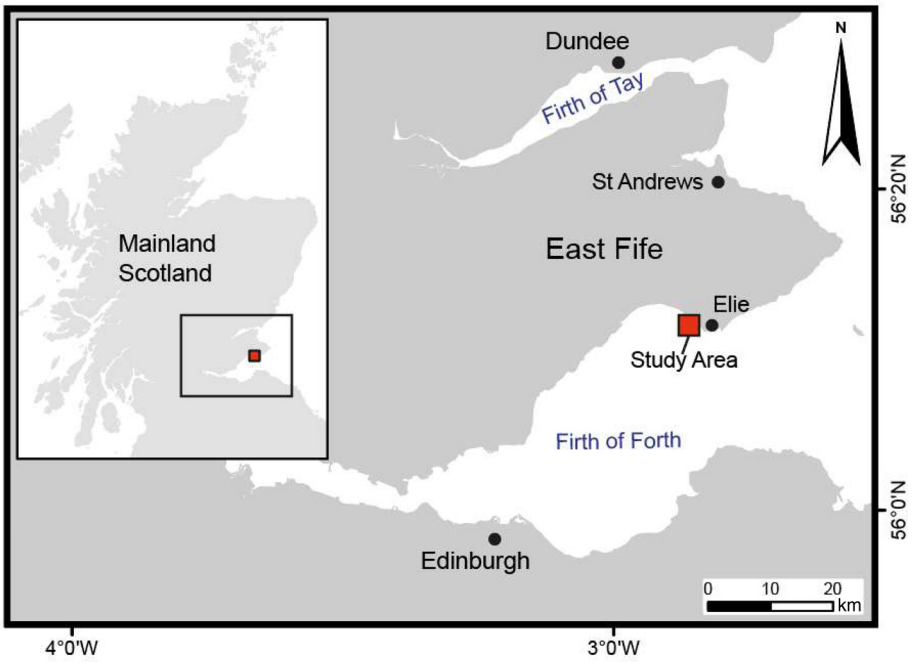

Fig. 2. Study site on the south coast of Fife. Basemap: GB National Outlines, 1:2 50 000, Contains public sector information licensed under the Open Government Licence v3.0. OS Open Data, EDINA supplied service, https://digimap.edina.ac.uk.

(Forsyth and Chisholm 1977). These Ruddons Point deposits were noted in as early as 1835, p. 181, when W. J. Hamilton remarked on their position, suggesting a 'subsequent elevatory movement has taken place' for them to be raised above sea-level. The raised deposits have an uneven surface due to erosion, wind-blown sand accumulation and vegetation cover but reach *c.* 6.7 mOD (metres above Ordnance Datum) at the coast and up to *c.* 9.5 mOD further inland. Mean high water spring (MHWS) tides across the field site reach *c.* 2.7 mOD, based on tidal records from the closest permanent tide gauge located at the Port of Leith (The National Oceanography Centre 2021). The deposits of

Fig. 3. (**a**) Aerial photography of study area. Locations of sample sites across study area are as follows: (1) Ruddons Point raised sand and gravel deposits; (2) core at mouth of Cocklemill Burn; (3) core in saltmarsh; (4) Cocklemill Burn raised sand and gravel deposits and core; (5) Cocklemill Burn core and approximate location of Overshott (2004) and Tooley and Smith (2005) sections. (**b**) Photograph of the raised shore platforms of Kincraig Point taken from east of Shell Bay looking south. Basemap: high resolution (25 cm) vertical aerial imagery © Getmapping Plc, EDINA supplied service, https://digimap.edina.ac.uk, downloaded: 2018-06-05 10:53:46.735.

Ruddons Point outcropping to the south of Largo Bay, and the underlying glacial till and clay have not previously been dated; however, research has been undertaken further inland along the Cocklemill Burn by Tooley and Smith (2005), and through an undergraduate dissertation by Overshott (2004), the results from which were presented in a field guide by Dawson and Dawson (2007). Tooley and Smith (2005) used radiocarbon dating on a sequence of the sediments, whereas Overshott (2004) focused on OSL. Both studies identified horizons that could be associated with the Main Postglacial Shoreline and Blairdrummond Shoreline, although the radiocarbon dates obtained by Tooley and Smith (2005) were generally older than the calculated OSL ages at similar elevations.

Figure 3 shows the sampling locations visited in the current study. This study aims to examine coastal change at five locations across the field site to expand upon the previous research conducted along the Cocklemill Burn and to further current understanding of the ice extent history and sea-level changes in this region of Scotland since the LGM. The raised deposits exposed on the coast at Ruddons Point (Locality 1) have not previously been dated. The raised terrace bank extends inland where deposits are exposed in section by a small river, the Cocklemill Burn, running through the field site. Deposits in this area, *c.* 0.5 km east of Locality 1, have previously been dated through Tooley and Smith's (2005) and Overshott's (2004) studies, however with differing results, and therefore these raised deposits were also investigated in this study, differentiated from the more coastal Ruddons Point section with the name Cocklemill Burn section and cores (Localities 4 and 5). The previous field studies by Overshott (2004) and Tooley and Smith (2005) were undertaken in the vicinity of Locality 5. Further coring was undertaken in two more sites within the study area, through clays close to the mouth of the Cocklemill Burn where it meets Largo Bay beach (Coastal Core, Locality 2) and in the saltmarsh adjacent to the raised deposits (Saltmarsh Core, Locality 3).

Methodology

Field methods

The field site preserves a complex depositional history with key features including: (1) ample examples of raised deposits composed of sand, shell and gravel horizons; (2) exposed glacial till and clay at the shore and exposed at the mouth of the Cocklemill river; and (3) preserved buried stratigraphy, including a basal peat, beneath the saltmarsh. To investigate each of these aspects of the field site, a multidisciplinary study was undertaken utilizing initial geological descriptions and geophysical investigation, followed by sampling for OSL profiling and dating, radiocarbon dating and complementary microfossil analyses, with the overarching aim of building a depositional interpretation and chronometric framework for the field site.

Geographical coordinates for each site location, as well as the elevation of each raised marine deposit section and the ground surface of each core location were keyed into Ordnance Survey (OS) elevations using a Trimble dGNSS, positioning system with a R8 Base and R6 Rover affixed to a 2 m antenna. Stratigraphic changes and sample locations were recorded relative to both its depth within the section or core, but also relative to Ordnance Datum Newlyn (mOD).

Detailed sedimentological descriptions were carried out on cleaned vertical sections through the deposits. Using a Wink vibracore drill system, four additional subsurface cores were collected to extend the sedimentological description into the subsurface and to allow for additional sampling. Magnetic susceptibility readings were taken at *c.* 5 cm intervals through 7.5 m of the Cocklemill Burn section using a handheld SM-30 magnetic susceptibility meter (ZH Instruments).

An electromagnetic (EM) ground conductivity survey was undertaken across the foreshore and saltmarsh adjacent to the raised deposits to improve understanding of the subsurface stratigraphy. The equipment used included the EM conductivity meter (CMD Explorer, GF Instruments) integrated with the Trimble dGNSS positioning system. The CMD Explorer was operated with coils in the vertical orientation and recording was set to continuous GPS measurement with *c.* 10 m line spacing between lines. The apparatus measures ground conductivity over three different depth ranges through the subsurface (C1 being the shallowest at approximate depth down to *c.* 2 m, C2 to *c.* 4 m and C3 the deepest to *c.* 6 m). To complement the EM ground conductivity survey, a direct current (DC) resistivity tomography line was acquired in a transect across the centre of the saltmarsh, using an ABEM SAS4000 Terrameter. The DC Resistivity method penetrates deeper into the subsurface than the EM conductivity survey with a maximum survey range of *c.* 12 m. Metal probes were positioned with 1 m spacing along a transect running broadly north–south through the site. The equipment automatically ran a series of iterations of potential resistivity between the probes to create a 2D electrical tomographic pseudo-section of the subsurface.

OSL sampling in the field

Sections 1 and 4, Ruddons Point and Cocklemill Burn, respectively, were profiled and sampled for OSL. Sections were first cut and cleaned by hand shovel, then covered with opaque black cover, with final cleaning taking place under this cover. For initial characterization, bulk sediment samples were taken at a high spatial sampling interval (5–15 cm between each sample) through each profile. These samples were subjected to rapid luminescence measurements using a SUERC portable OSL reader (Munyikwa *et al.* 2021). At Cocklemill Burn, additional samples were collected in small copper tubes for more targeted laboratory analysis. At Ruddons Point, samples for dating were collected by inserting steel tubes sealed with black tape, with corresponding dosimetry material for radionuclide concentration measurements. In-field gamma spectrometry was obtained at the Ruddons Point and Cocklemill Burn sections using a handheld Gamma Surveyor Vario (GF Instruments). Dating samples and associated dosimetry material were collected from the drilled cores under light-safe laboratory conditions.

Laboratory characterization

Simple laboratory screening of samples to assess luminescence sensitivities and approximate stored doses, then the

subsequent full OSL dating were carried out in the CERSA Luminescence Laboratory at the School of Earth and Environmental Sciences, University of St Andrews. Samples were opened in subdued red-light conditions and wet-sieved to isolate the 90–250 µm fraction. For initial laboratory screening, each sample underwent a hydrochloric acid (HCl) treatment for 10 minutes to remove carbonates, followed by a 40% hydrofluoric acid (HF) etch for 40 minutes to remove the outer surface of the grains, before a final HCl treatment for 10 minutes to remove fluoride precipitates. The grains were then dispensed to 10 mm diameter as *c.* 2 mm monolayer (small aliquot), greased, steel discs for loading into Risø TL-OSL DA-20 reader for analysis. For dating samples, grains underwent a heavy liquid (lithium polytungstate, LST) density separation to preferentially concentrate quartz grains, in addition to treatment with HCl, HF and HCl. The samples were re-sieved at 150 µm, and quartz dispensed in the 150–250 µm grain fraction.

A single aliquot regeneration (SAR) dose protocol was used to estimate equivalent doses (D_e) (Murray and Wintle 2000), with the protocol modified for CERSA423-427 to include a hot bleach at the end of the natural and regenerative dose cycles. Aliquots returning unacceptably high recuperation % or recycling ratios were rejected from further analysis. The central age model (CAM) (Galbraith *et al.* 1999) was used to calculate final D_e determinations for all samples.

Environmental dose rates for all dating samples were calculated from radionuclide concentrations (U, Th, K, Rb) measured by inductively coupled plasma mass spectrometry (ICP-MS), carried out within the University of St Andrews StAIG lab (ICP-MS) and Actlabs, Canada. Additionally, for the Ruddons Point section, high-resolution gamma spectrometry (HRGS) measurements were made on bulk sediment samples at the University of Stirling Environmental Radioactivity laboratories.

Radiocarbon analyses

A total of 10 radiocarbon dates were collected for analysis by accelerator mass spectrometry (AMS) at key horizons across the raised marine deposits and selected cores. All radiocarbon ages are presented in Table 1 in both conventional years BP and calibrated years BP. Calibrations have been carried out in the Calib Rev 8.1.0, using either the IntCal20 (Stuiver *et al.* 2021) or Marine20 (Heaton *et al.* 2020) calibration curves, and stated with one and two σ error ranges. All shells and shell fragments were calibrated using Marine20 calibration with a local ΔR of −141 ± 57, obtained from http://calib.org/marine/ (based on Harkness 1983) to compensate for the marine reservoir effect (MRE). Both humin and humic acid fractions of the peat sample were dated and calibrated using IntCal20. Five shell samples were submitted to BetaAnalytic, Miami, three shell samples were submitted to QUB CHRONO and one peat sample was submitted to SUERC for dating of both the humin and humic acid fractions.

Microfossil analysis

Microfossil analysis was undertaken on 19 samples from a 2.2 m interval through the raised sands of Ruddons Point

Table 1. *Radiocarbon results*

Sample ID (Lab ID)	Lab	Sample location	Height (mOD)	Material	Species	Age BP	Calibrated age BP (1σ range)	Calibrated age BP (2σ range)
RPS-UG1 (Beta-555074)	Beta Analytic	Ruddons Point (Locality 1)	Upper gravel *c.* 6.2	Shell	Gastropod, periwinkle	3130 ± 30	2813–3028 (1)	2738–3140 (1)
RPS-UB1 (Beta-555076)	Beta Analytic	Ruddons Point (Locality 1)	Upper gravel *c.* 5.9	Shell	Bivalve, cockle	3160 ± 30	2848–3067 (1)	2755–3171 (1)
RPS-LG1 (Beta-555075)	Beta Analytic	Ruddons Point (Locality 1)	Lower gravel *c.* 5.1	Shell	Gastropod, periwinkle	7200 ± 30	7537–7711 (1)	7447–7800 (1)
RudPtG1 (Beta-580486)	Beta Analytic	Ruddons Point (Locality 1)	Base of section above till *c.* 3.6	Shell	Gastropod (fragment)	7640 ± 30	7974–8156 (1)	7884–8266 (1)
RudPtBs (Beta-580485)	Beta Analytic	Ruddons Point (Locality 1)	Base of section above till *c.* 3.6	Shell	Bivalve (fragment)	7680 ± 30	8003–8190 (1)	7931–8300 (1)
CBS-SF1 (UBA-37101)	QUB CHRONO	Cocklemill Burn (Locality 4)	7.78	Shell	Bivalve, cockle	5449 ± 24	5688–5884 (1)	5585–5961 (1)
CBC-SF1 (UBA-37102)	QUB CHRONO	Cocklemill Burn (Locality 4)	1.85	Shell	Unknown (fragment)	8079 ± 28	8416–8620 (1)	8343–8766 (1)
CBC3-SF1 (UBA-37103)	QUB CHRONO	Cocklemill Burn (Locality 5)	1.77	Shell	Unknown (fragment)	8377 ± 28	8805–9051 (1)	8679–9181 (1)
CBC3-P1 (SUERC-93420)	SUERC	Cocklemill (Locality 5)	1.38	Peat	Humic acid	8225 ± 26	9127–9151 (0.19) 9168–9272 (0.81)	9029–9056 (0.07) 9085–9292 (0.93) 9389–9392 (0.003)
CBC3-P1 (SUERC-93424)	SUERC	Cocklemill (Locality 5)	1.38	Peat	Humin	8189 ± 25	9027–9058 (0.26) 9082–9139 (0.49) 9178–9200 (0.15) 9236–9252 (0.09)	9023–9147 (0.64) 9170–9270 (0.36)

All shell material was calibrated within the CALIB Rev 8.1.0 (Stuiver and Reimer 1993) using Marine20 (Heaton *et al.* 2020) and are reservoir corrected using a Local ΔR of −141 ± 57, available at: http://calib.org/marine/ (based on Harkness 1983). The peat samples were calibrated using IntCal20 (Reimer *et al.* 2020). All calibrated ages are expressed to both one and two sigma error ranges, with the probability of that age range presented in parentheses.

(Locality 1). Samples were broken into very small pieces by hand and put in a ceramic bowl to be thoroughly dried in an oven. They were then soaked in hot water with a spoonful of sodium carbonate added to help remove the clay fraction and facilitate release of the organic component. After soaking overnight, each sample was washed through a 75 µm sieve with hot water, the residue being decanted back into the bowl and dried. Because of the organic content of most of the clays/silts, this process had often to be repeated twice to achieve a good, clean breakdown. After breakdown and drying, the samples were stored in plastic bags and later picked of their microfaunal content under a binocular microscope. A selection of microfossils were picked out into faunal slides and recorded; the organic remains are recorded on a presence (x)/absence basis but the abundance of each ostracod and foraminiferal species is recorded semi-quantitatively (present/several specimens, common, etc.).

Results

Electrical and electromagnetic survey

The extent of the EM conductivity survey across the field area is presented in Figure 4. The surface represents results from the deepest penetration to depths of *c.* 6 m into the subsurface; however, the conductivity patterns show similar patterns at all three depths. Areas of higher conductivity (*c.* 300–400 mS m^{-1}) are identified in the central saltmarsh, and lower conductivity (between *c.* 0 and 250 mS m^{-1}) along the beach front and close to the edge of the raised terraces. The conductivity signature also appears to reduce as you move inland to the east. The conductive high in the central saltmarsh could be indicative of elevated levels of saline water within the saturated saltmarsh. Therefore, the survey results may be showing a gradual decrease in salt water as you move inland from the coast. The DC resistivity survey, running broadly south–north through the central saltmarsh (Fig. 5) shows that resistivity generally increases with depth and identifies a potential slope of the underlying sediments in a northerly direction, with the northerly slope most prominent in the resistivity bands ranging from *c.* 2.3 to *c.* 25.9 ohm-m (represented in green, yellow, gold and orange). The upper dark and light blue bands (*c.* 0.2 to 1.0 ohm-m) have no discernible slope, which suggests these represent saltmarsh sediments infilling over the underlying tilted sediments. The transition from saltmarsh silts into underlying sands and clays can also be seen in the core at Locality 3. The upper green resistivity bands (*c.* 2.3 ohm-m) outcrop at surface level at the southern end of the transect, which suggests that this could be representative of the diamict and clays which also outcrop at the coast and therefore may continue beneath the saltmarsh and dip in a northerly direction. The lowest red band (resistivity of >25.9 ohm-m) does not exhibit a tilt towards the north and therefore may represent the underlying bedrock geology. The DC resistivity transect also reveals the presence of a depression in the resistivity layers, which is interpreted as an infilled palaeo river channel running through the field site.

Locality 1: Ruddons Point raised marine deposits

Description

The Ruddons Point terrace has a large cut bank exposure along the modern shoreface to the south of Largo Bay (Fig. 6). At the base of the exposed raised deposits is a glacial till, which extends below the modern beach level. The soft, fine-grained, grey clay matrix contains angular clasts of various lithologies. The till unit appears to pinch out towards the NE as you move laterally along the exposure. Deposited on top of the till is >3 m of sand and gravel and cobble units (*c.* 3.57–6.77 mOD). The lowest *c.* 0.60 m of sand is dark brown in colour, fine grained and organic rich, with evidence of burrowing and bioturbation. There is also evidence of thin (*c.* 1–2 cm thick) gravel horizons within the sand. The darker

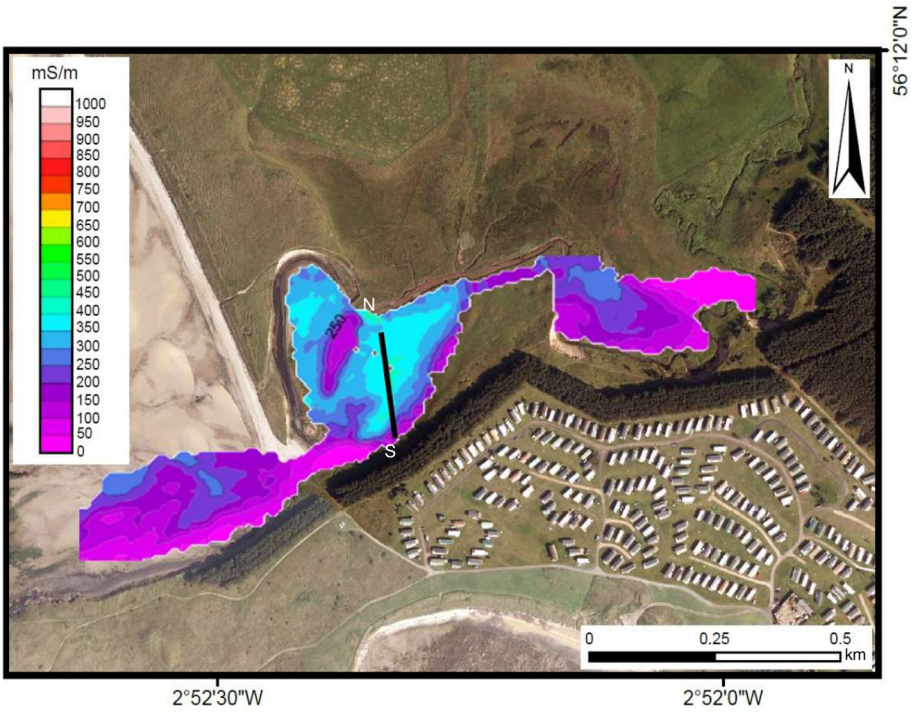

Fig. 4. Electromagnetic (EM) Conductivity survey results (*c.* 6 m depth) superimposed on to aerial photography of field area. Black line orientated approximately north–south through central saltmarsh indicates the position of direct current (DC) resistivity survey. Basemap: high resolution (25 cm) vertical aerial imagery © Getmapping Plc, EDINA supplied service, https://digimap.edina.ac.uk, downloaded: 2018-06-05 10:53:46.735.

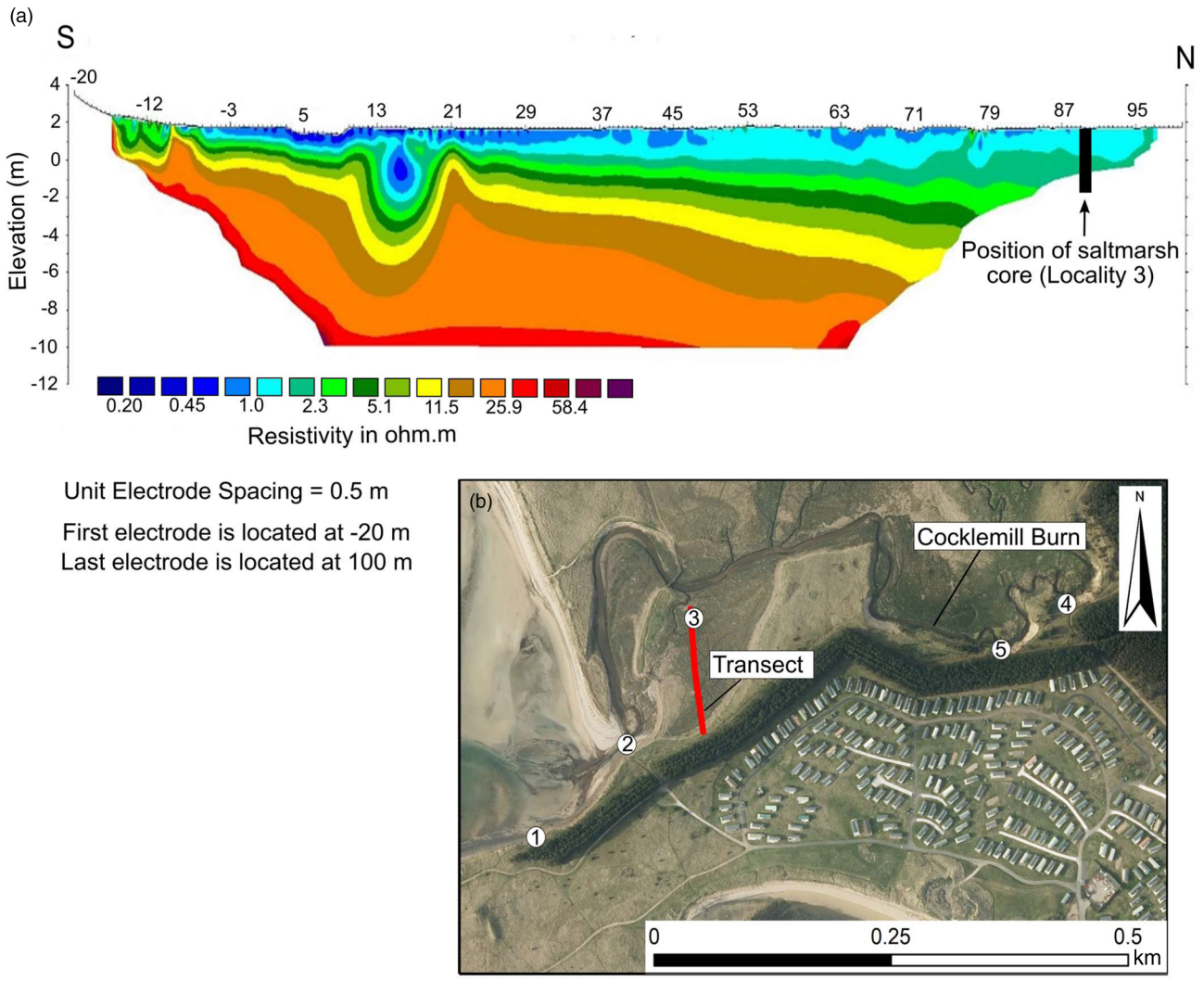

Fig. 5. (**a**) Direct current (DC) resistivity model of the subsurface, created using RES2DINV (Geotomo Software). Position of saltmarsh core labelled towards northern end of transect. (**b**) Position of the transect within wider study area and in relation to other studied localities. Basemap: high resolution (25 cm) vertical aerial imagery © Getmapping Plc, EDINA supplied service, https://digimap.edina.ac.uk, downloaded: 2022-05-08 17:08:48.323.

sand transitions at *c.* 4.17 mOD to a lighter beige sand unit (*c.* 0.70 m in thickness) with less evidence of disturbance. The upper 0.12–0.15 m of this unit is laminated. A sharp contact separates these sands from the overlying unit of cobble-sized clasts, which is *c.* 0.45 m thick, although the thickness is variable along strike in the exposure. This gravel and cobble horizon is supported by a coarse sand matrix that contains heavily weathered molluscs. Individual clasts are sub-rounded, the largest being *c.* 18–20 cm in the longest axis, and are comprised predominantly of igneous and metamorphic lithologies such as basalt and quartzite. Overlying this unit is a light beige fine sand, *c.* 0.35 m in thickness, and at *c.* 5.67 m OD, the sand transitions to a darker beige, *c.* 0.25 m in thickness. Another sharp contact separates this sand from an overlying gravel unit. The average clast size is smaller than the lower unit, which contains both gravel and cobble-sized clasts. The unit has an abundance of marine shells, including intact limpet, periwinkle, cockle and razor clam shells. In some areas of the exposure, there appears to be an imbrication in the gravel and cobbles in an easterly direction. Directly above this gravel, at *c.* 6.20 m is a shell-supported unit, *c.* 0.10 m in thickness, containing numerous whole, unbroken shells, predominantly gastropods (periwinkle). The uppermost stratum of the section is a cap of modern sandy soil until the surface at 6.77 mOD, with prevalent root systems throughout, which is variable in thickness.

OSL chronology

Initial in-field screening of the sands suggests a slight increase in net OSL and infra-red stimulated luminescence (IRSL) intensities with depth through the section, with the exception of the lowest part that consists of darker, bioturbated sands. The darker sands show an initial inversion to lower signal intensities between *c.* 4.20 and 3.80 mOD. Below this, intensities again increase with depth, through the lowest *c.* 0.25 m of the section, between *c.* 3.80 and 3.55 mOD. OSL and IRSL depletion return the lowest values in the sands directly below the overlying gravel units as well as in the darker sands at the base of the section. The ratio of IRSL: OSL is also variable through the section, ranging from *c.* 0.10 in the darker sands of the lowest 0.60 m of the section to *c.* 0.19 in the sands between the gravel units (Fig. 7). Subsequent laboratory analyses suggest a less complex depositional sequence, with a slight increase in stored dose with depth; this

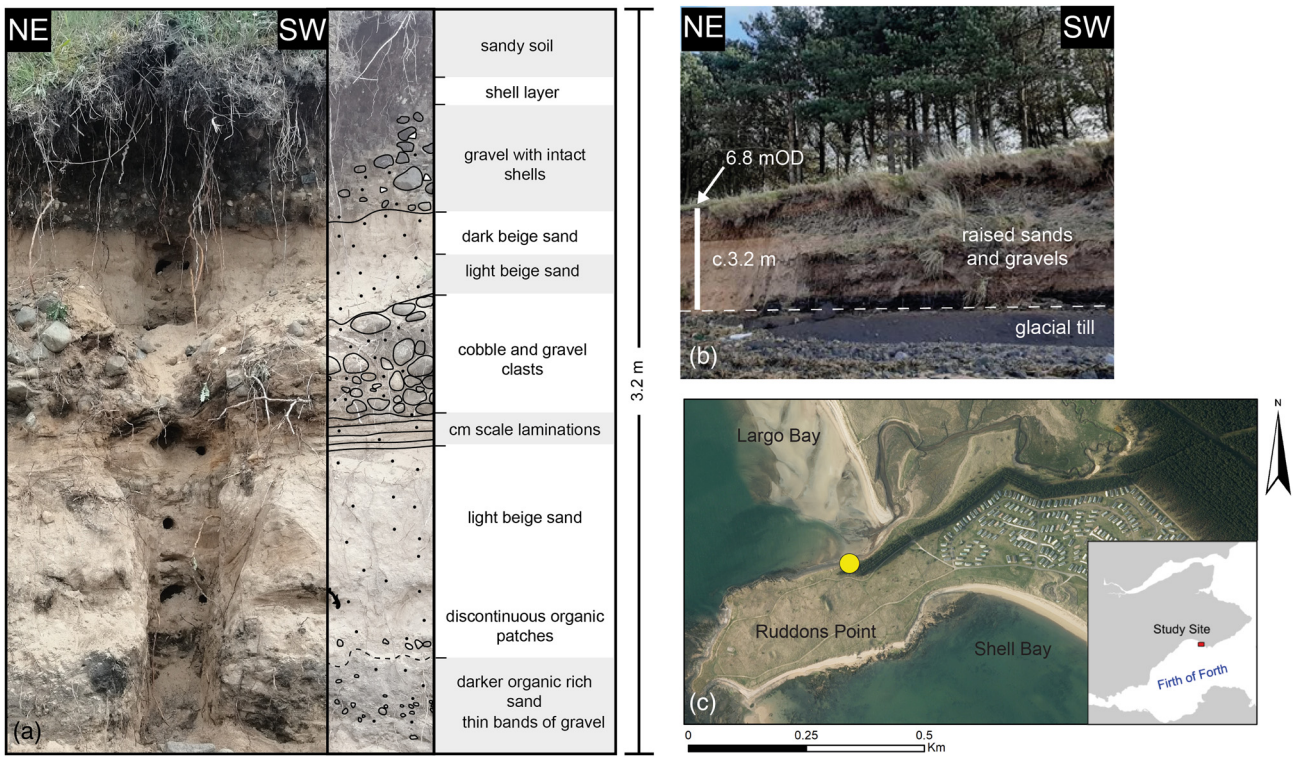

Fig. 6. Ruddons Point (Locality 1). (**a**) Photograph of sand and gravel deposits; (**b**) photograph showing exposed glacial till below sand and gravel deposits; (**c**) position of Locality 1 within field study area. Basemap: high resolution (25 cm) vertical aerial imagery © Getmapping Plc, EDINA supplied service, https://digimap.edina.ac.uk, downloaded: 2022-05-08 17:08:48.323.

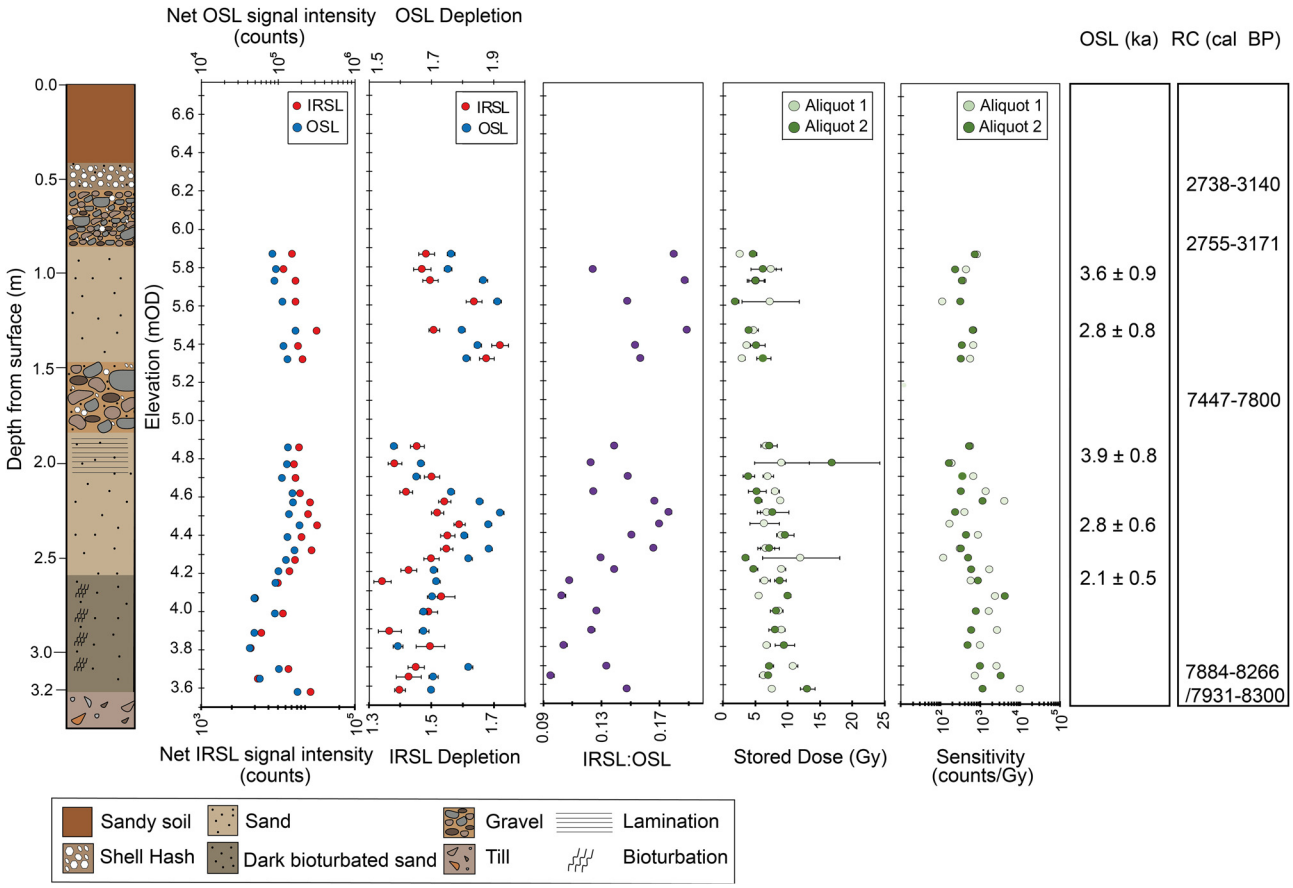

Fig. 7. Luminescence profiling and optically stimulated luminescence (OSL) (ka) and radiocarbon (RC) (cal years BP, 2σ error ranges) ages for the Ruddons Point raised marine deposits (Locality 1).

suggests that the reduction in OSL and IRSL intensities through 4.20–3.80 mOD above is partly influenced by grain colour. The paired stored dose estimates are often divergent, suggesting for the most prominent of these that the sediment was poorly bleached at deposition.

All OSL ages are presented in Table 2. Five OSL dating samples were collected through the section, in each of the sand units. The sample highest in the sequence yielded an OSL date of 3.57 ± 0.88 ka (at 5.77 mOD), with the underlying sample dated to 2.75 ± 0.78 ka (at 5.44 mOD). Below the lower gravel the three OSL samples also show an age inversion with depth, dated to 3.87 ± 0.77 ka (4.78 mOD), 2.75 ± 0.59 ka (4.45 mOD) and 2.06 ± 0.49 ka (4.17 mOD), with the lowest sample taken just above the transition from the beige sands to the darker sands below. The error ranges of the upper four measurements overlap and have a weighted combined age of 3.14 ± 0.37 ka. The lowest sample in the section is potentially underestimating the depositional age.

Radiocarbon chronology

Through the Ruddons Point raised marine deposits, five marine shell samples were radiocarbon dated; two from the upper gravel, one from the lower gravel, and a further two shells from the base of the section, above the glacial till (conventional and calibrated dates presented in Table 1). Dated shells from the upper gravel returned comparable ages 2738–3140 cal years BP and 2755–3171 cal years BP (all dates reported with 2σ age range). These dates would suggest deposition of the gravel shortly deposition of the lower sands (dated above to 3.14 ± 0.37 ka). From the lower gravel, a bivalve dated to 7447–7800 cal years BP. This is at odds with the younger OSL ages surrounding this gravel horizon. This might suggest the shell was redeposited during the high-energy deposition of the gravel. The shell was largely intact, which suggests that it was not transported far. Shell fragments collected from the base of the section above the till are dated to 7884–8266 and 7931–8300 cal years BP.

Microfossil analyses

Results from the microfossil analyses are displayed in Table 3. The lowermost microfossil samples collected from the Ruddons Point profile section (at 3.60–3.00 m depth, *c.* 3.50–4.10 mOD) indicate the sediment is an inhospitable environment for the microfauna, because within these samples only coal/charcoal, megaspores and plant debris were identified. A slight exception, at 3.30 m depth, there were very rare quantities of marine molluscs and ostracods. At 2.90 m foraminifera were identified, including *Ammonia batavus*, *Cibicides lobatulus*, *Elphidium macellum*, *Planorbulina mediterranensis* and *Elphidium margaritaceum*. All samples collected above 2.80 m depth within the section were considered to represent a more hospitable environment for microfauna, with common and diverse microfauna, derived from marginal marine and inner shelf environments, found in all of the samples from 2.8–1.40 m depth (*c.* 4.30–5.70 mOD). The samples collected within the beige sands beneath the lower gravel in the profile (samples from 2.80–2.00 m depth, *c.* 4.30–5.10 mOD) are shelly and contain small molluscs (bivalves, barnacle and echinoderm fragments). The identified foraminifera would have lived on or attached to hard substrates. A commonly identified foraminifera within the samples is *C. lobatulus*, which is listed by Murray (2006, p. 333) under shelf environments as

Table 2. *OSL results*

Sample ID (Lab ID)	Depth (m)	Aliquots accepted (total measured)	Water content (%)	CAM D_e (Gy)	σd (%)	Beta Ḋ* (Gy ka^{-1})	Gamma† Ḋ (Gy ka^{-1})	Cosmic Ḋ (Gy ka^{-1})	Environmental Ḋ (Gy ka^{-1})	Age (ka)
Ruddons Point (Locality 1)										
CERSA423	1.00	18 (24)	16 ± 5	2.26 ± 0.20	36 ± 7	0.30 ± 0.12	0.18 ± 0.08	0.16 ± 0.02	0.63 ± 0.15	3.6 ± 0.9
CERSA424	1.33	16 (24)	14 ± 5	2.09 ± 0.29	49 ± 11	0.37 ± 0.13	0.23 ± 0.14	0.15 ± 0.02	0.76 ± 0.19	2.8 ± 0.8
CERSA425	1.99	16 (23)	18 ± 5	3.75 ± 0.54	51 ± 11	0.53 ± 0.10	0.30 ± 0.08	0.14 ± 0.01	0.97 ± 0.13	3.9 ± 0.8
CERSA426	2.32	22 (24)	18 ± 5	2.67 ± 0.21	34 ± 6	0.56 ± 0.14	0.28 ± 0.14	0.14 ± 0.01	0.97 ± 0.20	2.8 ± 0.6
CERSA427	2.60	15 (18)	17 ± 5	1.91 ± 0.22	43 ± 9	0.53 ± 0.14	0.27 ± 0.13	0.13 ± 0.01	0.93 ± 0.19	2.1 ± 0.5
Coastal Core (Locality 2)										
CERSA447	1.18	24 (24)	19 ± 2	72.62 ± 3.27	21 ± 3	1.52 ± 0.04	0.91 ± 0.03	0.16 ± 0.02	2.59 ± 0.05	28.1 ± 1.4
Saltmarsh Core (Locality 3)										
CERSA445	2.63	21 (24)	24 ± 5	47.67 ± 3.03	28 ± 5	1.62 ± 0.05	0.83 ± 0.04	0.13 ± 0.01	2.58 ± 0.07	18.5 ± 1.3
CERSA446	3.37	20 (20)	21 ± 7	83.84 ± 8.86	46 ± 8	1.81 ± 0.06	0.95 ± 0.05	0.12 ± 0.01	2.88 ± 0.08	29.1 ± 3.2
Cocklemill Burn (Locality 4)										
LL2	0.89	10 (15)	17 ± 5	0.25 ± 0.04	-	0.51 ± 0.08	0.22 ± 0.09	0.16 ± 0.02	0.90 ± 0.16	0.3 ± 0.1
LL7	2.01	13 (20)	17 ± 5	3.54 ± 0.20	12 ± 6	0.46 ± 0.09	0.22 ± 0.19	0.14 ± 0.01	0.82 ± 0.23	4.3 ± 1.2
LL12	2.23	15 (21)	17 ± 5	4.44 ± 0.22	13 ± 5	0.44 ± 0.07	0.21 ± 0.08	0.14 ± 0.01	0.80 ± 0.14	5.6 ± 1.0
LL14	3.00	18 (22)	17 ± 5	4.28 ± 0.16	12 ± 3	0.58 ± 0.07	0.25 ± 0.08	0.12 ± 0.01	0.96 ± 0.14	4.5 ± 0.7
LL19	4.30	19 (24)	17 ± 5	7.46 ± 0.22	10 ± 2	0.60 ± 0.17	0.27 ± 0.17	0.11 ± 0.01	0.97 ± 0.30	7.7 ± 2.4
LL20	4.60	19 (22)	17 ± 5	6.00 ± 0.28	19 ± 4	0.58 ± 0.11	0.25 ± 0.12	0.10 ± 0.01	0.94 ± 0.21	6.4 ± 1.5
LL22	5.65	22 (24)	17 ± 5	5.40 ± 0.20	17 ± 3	0.60 ± 0.17	0.27 ± 0.17	0.09 ± 0.01	0.96 ± 0.30	5.6 ± 1.8
CERSA473	2.15	15 (26)	30 ± 1	4.88 ± 0.18	9 ± 4	0.43 ± 0.05	0.24 ± 0.04	0.14 ± 0.01	0.81 ± 0.06	6.0 ± 0.5
CERSA473 – corrected	2.15	15 (26)	30 ± 1	4.88 ± 0.18	9 ± 4	0.41 ± 0.05	0.23 ± 0.04	0.14 ± 0.01	0.78 ± 0.06	6.3 ± 0.5

All results reported to two decimal places, with calculations made prior to rounding. Dates are relative to the years 2019/20. CAM, central age model.
*Attenuated for grain size based on Mejdahl (1979).
†Reconciled lab gamma and field gamma where available.

Table 3. *Microfossil analyses undertaken on samples from Ruddons Point (Locality 1)*

Depth in profile (m)	1.4	1.5	1.6	1.7	2.0	2.1	2.2	2.3	2.4	2.5	2.6	2.7	2.8*	2.9	3.0	3.1	3.2	3.3	3.6
Marine molluscs	x	x	f	x	x	x	x	f	x	x	x	x	x	f				r	
Outer estuarine/marine foraminifera	x	r		x	x	x	x	x	x	x	x	x	x	x					
Barnacle debris	x	x	f	x	x	x	x	x	x	x									
Outer estuarine/marine ostracods	r			r	x	x	x	x	x	x	x	x	x					r	
Plant debris		x	x		x	x	x			x	x				x	x	x		
Iron mineral			x																
Echinoderm debris					x	x	x	x	x	x	x	x							
Coal/charcoal + megaspores						x				x	x	x	x	x	x	x	x	x	x
Sediment	*coarse sandy silt*								*shelly*							*coal*			*coal*
	UPPER SAND									*LOWER SAND*									*TILL*

Contained material is recorded on a presence (x)/absence basis; r – very rare; f – fragments only. Samples collected <5 m laterally from OSL sampling location, with the upper and lower sand units correlating to the upper and lower sands in the Ruddons Point sedimentary log. Exact depth in profile will vary depending on variable surface height.
*First common microfossil.

'epifaunal; usually attached and immobile, especially in high energy'. It tends to be attached to stones, pebbles or marine algae. Others cling to marine algae (e.g. *Ammonia batavus*, *Elphidium* spp.) in the littoral/sublittoral of marginal marine environments. There are no miliolids present in any of the samples.

Ostracods which have been identified within the samples include *Hemicythere villosa*, *Leptocythere pellucida*, *Cythere lutea*, *Cytheropteron* spp., *Palmoconcha guttata*, *Paracytheridea cuneiformis*, *Robertsonites tuberculatus*, *Sarsicytheridea bradii*, *Semicytherura undata*, *Finmarchinella angulate*, *Finmarchinella finmarchica*, *Hemicytherura clathrate* and *Aurila convexa*. The ostracods are marginal marine/inner shelf species (either phytal or sediment dwelling), from which habitats they were washed into the sand deposits of Ruddons Point.

Locality 2: coastal core

Core description

The coastal core was driven through till close to the mouth of the Cocklemill Burn (Fig. 8). The core reached a depth of 1.27 m from 2.23–0.96 mOD. There are no lithic fragments and only sparse amounts of shell fragments within the core. The clay within the bottom *c.* 0.20 m of the core contains noticeably less sand than the sediment above and is noticeably more plastic. Overlying this clay, is a fine, well-sorted light beige sand horizon, *c.* 6–7 cm thick (1.80–1.74 mOD). The contacts between this sand layer and the clays above and below it are sharp. The overlying clay is dark grey-brown sandy clay with a lack of any lithic fragments. The topmost 0.11 m of the core is a dark brown, fine-grained, organic-rich sediment (Fig. 9).

OSL chronology

Initial field-based OSL screening revealed that the upper most sediment (top *c.* 0.11 m) had distinctly lower OSL and IRSL signal intensities than the sediments below, suggesting a discontinuity in age between the surface sediments, which could have been significantly reworked and bleached by both coastal and fluvial processes. This trend was reproduced in the subsequent laboratory characterization, with the paired aliquots from the three uppermost samples returning a small stored dose compared to the samples from the underlying sediments. A full dating sample was collected from close to the base of the core at 1.05 mOD (CERSA447) and OSL dated to 28.09 ± 1.37 ka, with an over dispersion (σd) of 21 ± 3% (Table 2). Over dispersion is a measure of variability in the calculated equivalent dose (D_e). An example of the OSL signal and regenerative curve for an aliquot within the sample is shown in Figure 10. No samples were collected for radiocarbon dating within this core.

Locality 3: saltmarsh core

Core description

The saltmarsh core was collected through the intertidal saltmarsh which infills the lowlands at approximately high tide level. The core extended to a depth of 3.57 m, between 2.71 and −0.86 mOD and reveals both clay- and sand-rich horizons (Fig. 11). The lowermost 0.33 m of the core consists of a sandy brown clay with rounded to sub-rounded pebbles up to 1 cm in length and evidence of small coal fragments. Overlying this is a lithic sand with coarse to very coarse lithic fragments and medium-grained sand which fines upwards through the core. This lithic sand has a grey-blue colour which transitions to a brown-green coloration at *c.* 1.10 mOD. At *c.* 0.70–0.45 mOD there is a brown clay horizon within the sand with millimetre-scale, sub-rounded lithics, and centimetre-scale gravel. The sand overlying this sand is dark brown/beige and contains shell fragments and small lithic fragments. Above this is a coarse, black, highly organic layer (*c.* 6 cm thick) and the uppermost *c.* 1.00 m consists of a dark brown, fibrous and waterlogged saltmarsh clay with a high organic content. The clay contains a small amount of angular shell fragments (<2%) and an absence of sand and pebbles.

OSL chronology

Initial rapid screening of the core using portable OSL displayed an overall increase in OSL and IRSL net signal intensities with depth, suggesting an age progression within the core (Fig. 11). To ascertain the age of the lowest sediment in the sequence, which is also the lowest elevation sediment cored in the field study, a dating sample was collected from the lowermost clay (CERSA446 at −0.66 mOD). A second sample was collected from the lithic sand stratigraphically above the clay (CERSA445 at 0.08 mOD) to explore the age range between the clay and overlying sand. Results show that

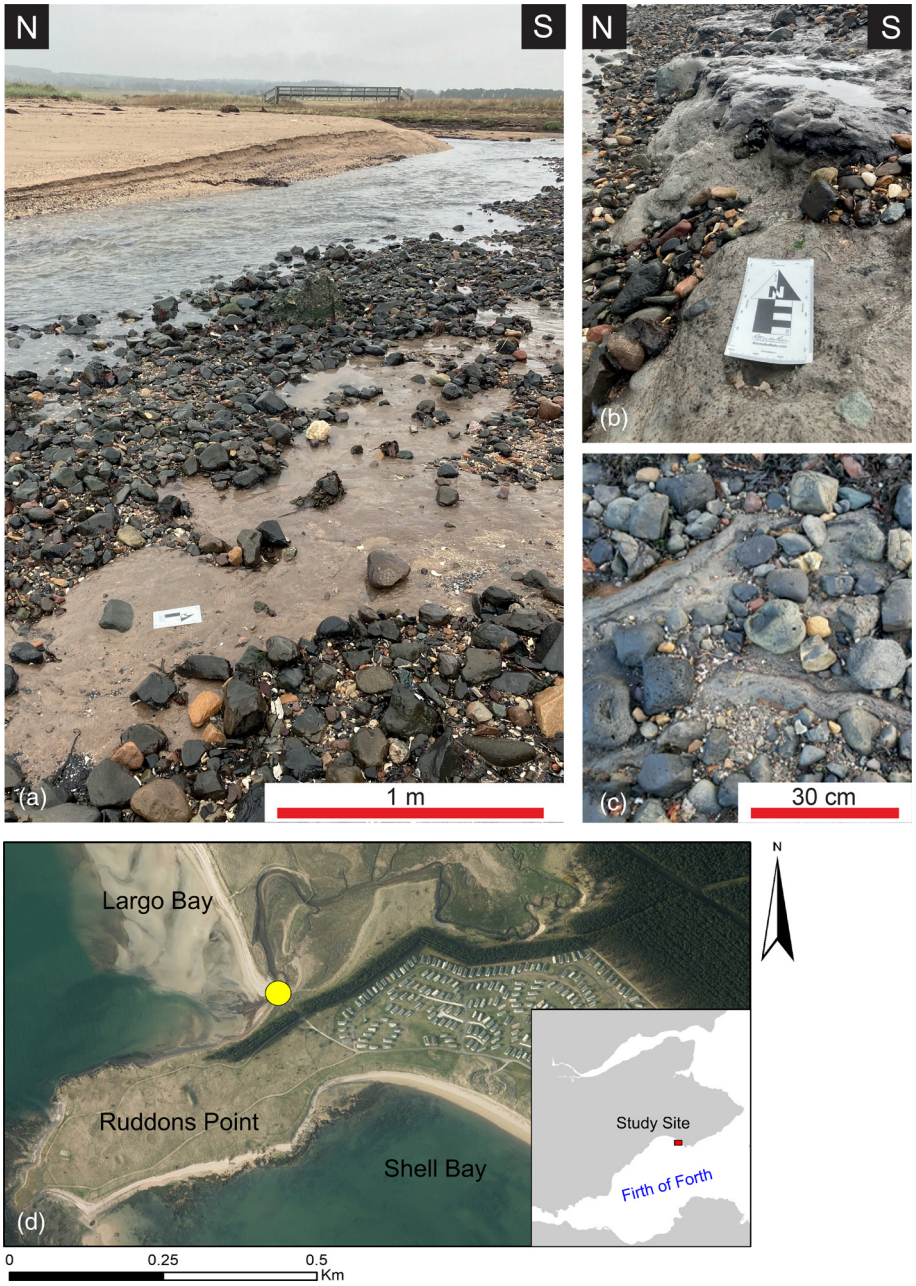

Fig. 8. Panel of field photographs of coastal clays. (**a**) Clays exposed beneath beach cobbles at the mouth of the Cocklemill Burn; (**b**) clays exposed by the river, showing a darker upper clay cap under which is a lighter blueish-grey clay with angular clasts. (**c**) Example of potential ice push structures on the exposed clay; (**d**) position of Locality 2 within field study area. Basemap: high resolution (25 cm) vertical aerial imagery © Getmapping Plc, EDINA supplied service, https://digimap.edina.ac.uk, downloaded: 2022-05-08 17:08:48.323.

the lithic-rich sand of CERSA445 date to 18.51 ± 1.28 ka, and the underlying clay to 29.12 ± 3.18 ka. The σd within the lithic sand is 28 ± 5% but is much higher in the underlying clay at 46 ± 8%. In this situation there is no evidence of bioturbation; however, there is potential for either incomplete bleaching at the point of deposition or the presence of numerous lithic fragments and pebbles within the clay could be causing variability in the beta dose rates.

Locality 4: Cocklemill Burn raised marine deposits and cores

Sedimentological description

The Cocklemill Burn raised deposits are composed of sands, gravels, organic-rich layers containing coal fragments, and shell hash horizons, topped by windblown sands and sandy soil (Fig. 12a). The base of the section from *c.* 1.78–2.38 mOD displays cycles of poorly sorted, medium to coarse sands and units of well-rounded gravels (*c.* 2–4 cm in size) with lithologies of sandstones, basalt and quartz. Between the gravel-rich units is a 2–3 cm thick bed of coarse-grained organic-rich material and a coarse-grained sand. Overlying the gravels, from 2.38–2.63 mOD are medium to coarse-grained sands with organic matter in discontinuous layers.

From *c.* 2.63–2.98 mOD area a series of sand beds, which display flaser bedding with visible lenses of darker, coarser material. They do not form a continuous layer and are laterally variable. There are a scattering of larger centimetre-scale pebbles and shell fragments visible within the sands. From 2.98–3.63 mOD are interbedded sands with numerous centimetre-scale gravel beds topped by a gravel bed, *c.* 0.15 m thick, with rounded clasts (ranging from 1–3 cm in scale). Above the gravels, from *c.* 3.63–4.83 mOD the sands are fine to medium grained, with further occurrence of a thin (2 cm thick) black organic layer and thin (2–5 cm thick) gravel beds. Occasional orange iron staining within the sands is associated with infilled burrows and dark patches of

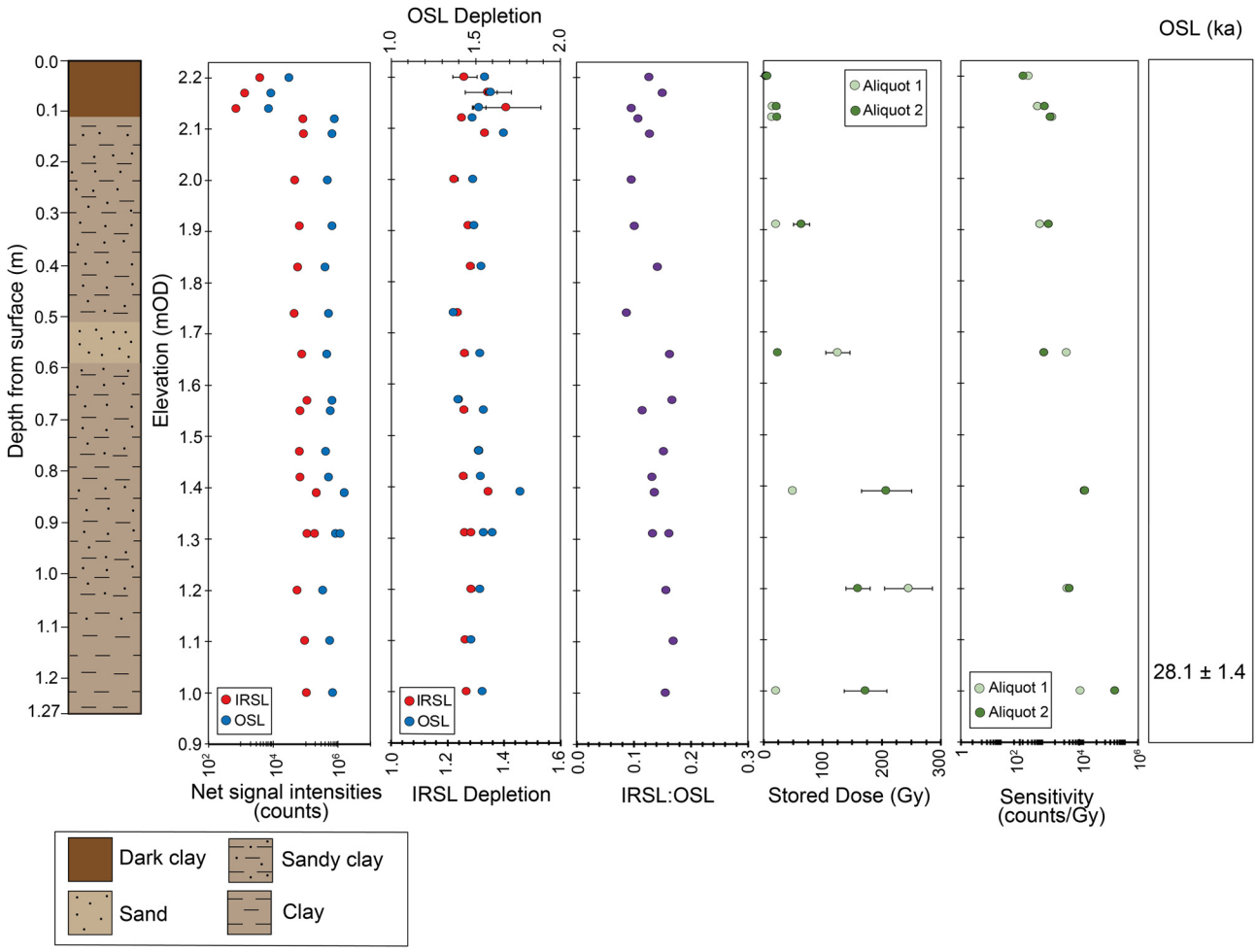

Fig. 9. Luminescence profiling and optically stimulated luminescence (OSL) (ka) age for the coastal core (Locality 2).

organic material. There are also irregularly occurring pebbles and shell fragments within the sands. At *c.* 4.83–5.03 mOD is a gravel and shell hash bed *c.* 0.20 m thick. The sands above this shell/gravel bed (5.03–7.73 mOD) contain shell fragments, with cycles of shell-rich beds. The sand units show further evidence of burrowing and horizons of heavy bioturbation infilled by dark organics. The uppermost horizons of the marine deposits, from 7.73–8.03 mOD, consist of shell hash and an organic coal-rich layer which varies in thickness laterally across the section. This manifests

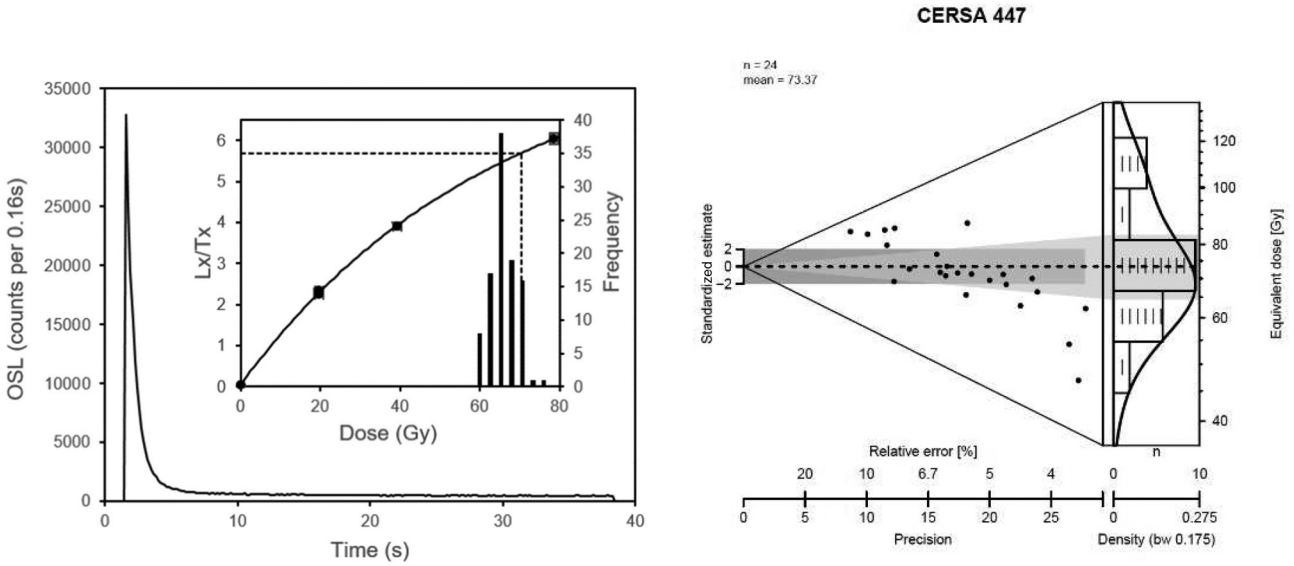

Fig. 10. (**a**) Example optically stimulated luminescence (OSL) signal and growth curve for CERSA447, Disc48. (**b**) Example Abanico Plot (Dietze *et al.* 2016) for CERSA447 where all 24 measured aliquots were accepted (plotted using ShinyPlot).

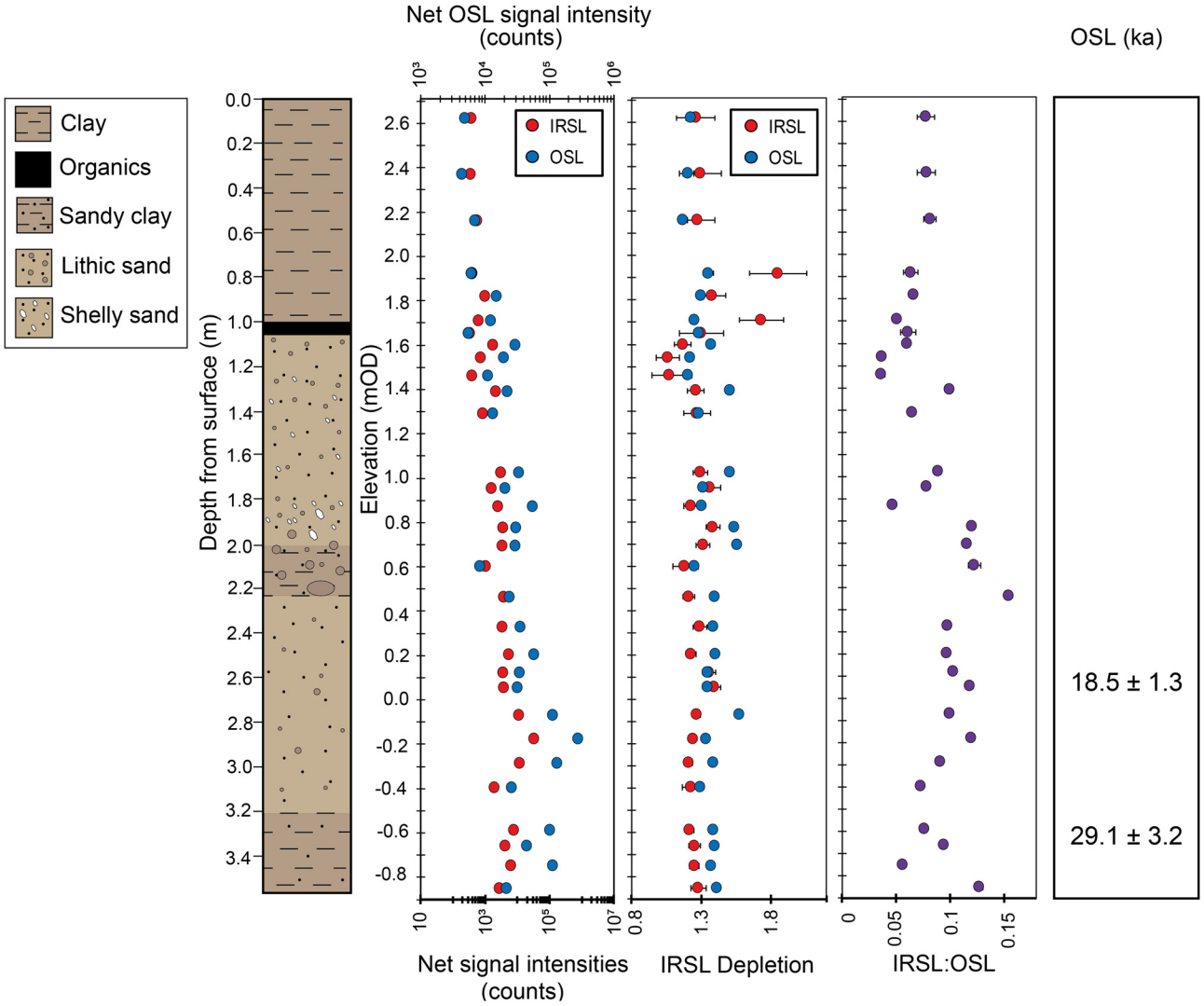

Fig. 11. Luminescence profiling and optically stimulated luminescence (OSL) (ka) ages for the saltmarsh core (Locality 3).

as two thin distinct coal bands but when followed laterally it combines with a shell hash layer to form a thicker band of shell fragments, larger whole shells and fine and centimetre chunks of coal fragments. From *c.* 8.03–9.34 mOD are fine to medium sands with evidence of shell fragments and many modern roots within the sands.

The core taken at the base of the section at Locality 4 spans a depth of 2.45 m, from 2.64–0.19 mOD. The bottom *c.* 1.60 m contains sand with discontinuous organic-rich layers. Above this is a shell horizon, followed by *c.* 0.80 m of sand with thin gravel layers. The second Cocklemill core taken at Locality 5, *c.* 80 m to the west, spans a depth of 1.22 m, from 2.56–1.34 mOD. At the base of the core is a dark brown, compacted, friable peat, above which is a soft, grey-coloured, carse clay. The carse clay and peat were not noted in the Cocklemill core at Locality 4, despite recording sediments at a similar elevation. Above the carse clay is a medium-grained sand containing angular shell fragments and discontinuous organic-rich bands, but no lithic fragments, similar to the sediments in the core at Locality 4. A thin (1–2 cm thick) shell layer, 0.80 m from the top of the core, separates sands which are grey-beige in colour from more orange-beige sands above it.

OSL chronology

A step-change in IRSL and OSL net signal intensities occurs across a break at *c.* 1.35 m depth (8.04 mOD), with the intensities increasing by two orders of magnitude (Fig. 13). This trend was reproduced in the subsequent laboratory screened OSL dataset with the stored dose 'jumping' from sub-Gy to *c.* 5 Gy. Moving further down the section, the stored doses from *c.* 1.50 to *c.* 3.14 m depth are in the region of *c.* 4–6 Gy, after which the stored dose appears to broadly increase with depth until *c.* 4.60 m (*c.* 4.74 mOD), after which point the stored dose drops off from *c.* 10 to *c.* 6 Gy for the rest of the section. This implies that the environmental dose rates are different above and below the depth of 4.60 m, or that there is a difference in luminescence sensitivities, which could reflect variations in characteristics such as mineralogy or grain size.

The uppermost OSL dating sample (LL2) was taken at 0.89 m depth from the top of the section (8.45 mOD) and provided a date for the upper sand of 0.28 ± 0.07 ka. This young age corroborates the results from the field-based measurements of OSL and calibrated OSL screening, which identified lower signal intensities and stored dose in the upper sands of the section. The next three samples; LL7 at 2.01 m depth (7.33 mOD), LL12 at 2.23 m depth

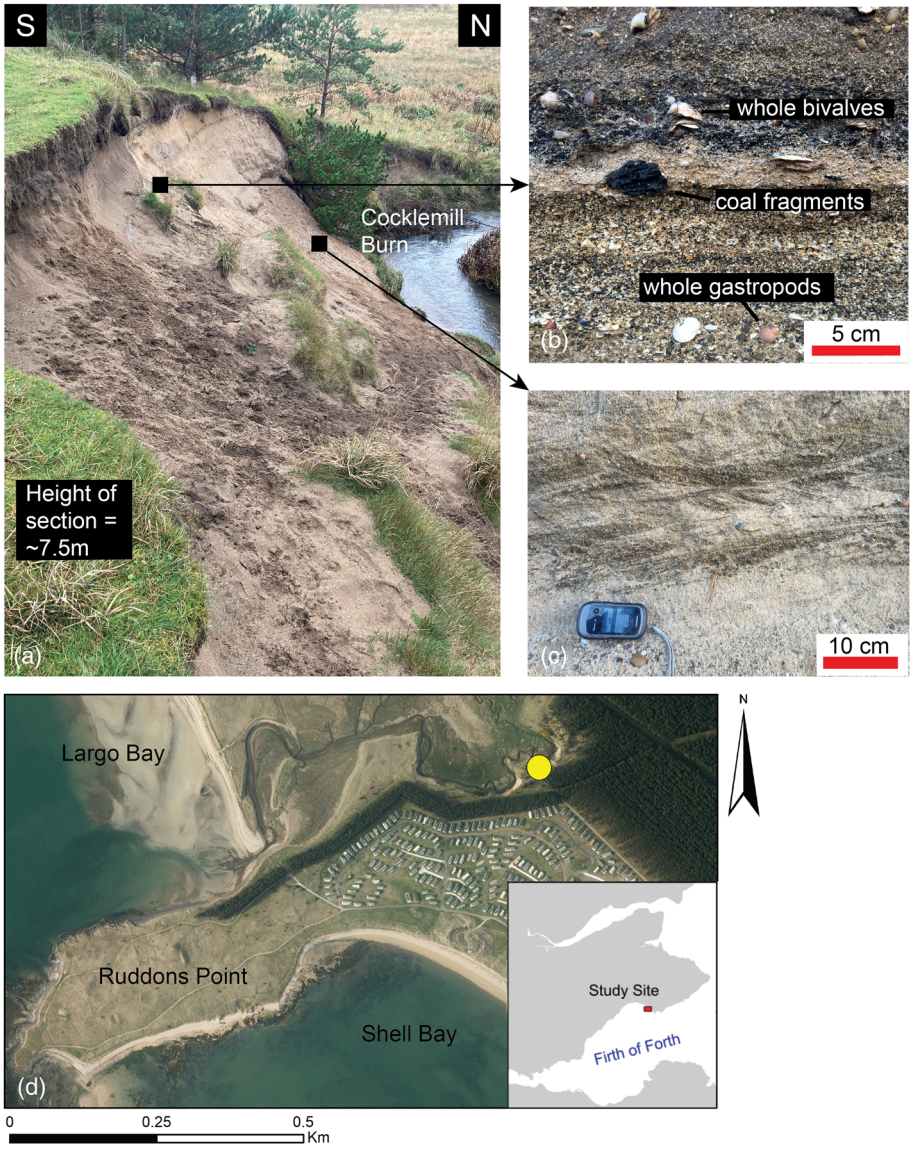

Fig. 12. Panel of field photographs to illustrate stratum descriptions. (**a**) Cocklemill Burn raised marine deposit, incised by the Cocklemill Burn [British National Grid Reference: 346257 700888]; (**b**) uppermost shell- and coal-rich horizon with intact bivalve and gastropod shells and centimetre-scale coal fragments; (**c**) photograph showing flaser bedding where ripples are picked out in the cross beds by the separation of gravels within the coarse sand; (**d**) position of Locality 2 within field study area. Basemap: high resolution (25 cm) vertical aerial imagery © Getmapping Plc, EDINA supplied service, https://digimap.edina.ac.uk, downloaded: 2022-05-08 17:08:48.323.

(7.11 mOD) and LL14 at 3.00 m depth (6.34 mOD) in the section were dated to 4.34 ± 1.24 ka, 5.58 ± 0.99 ka, and 4.46 ± 0.66 ka, respectively, with a combined age of 4.73 ± 0.50 ka. OSL sample LL19 at 4.30 m depth (5.04 mOD) was dated to 7.66 ± 2.38 ka, although it has a large associated error. This sample was taken above the break in stored dose identified in the calibrated OSL results and also coincides with a change in magnetic susceptibility readings. The lower section yielded two younger ages of 6.41 ± 1.45 ka (LL20, 4.74 mOD) and 5.63 ± 1.77 ka (LL22, 3.69 mOD). Initial OSL screening of both of the cores at Locality 4 and Locality 5 did not show an obvious increase in signal intensity with depth (Figs 14 and 15). Likewise, there was no noticeable increase in stored dose through the calibrated OSL in the core at Locality 4. At Locality 4, a full dating sample (CERSA473) was taken near the base of the core, at an elevation of 0.49 mOD, which yielded an age of 6.02 ± 0.53 ka. These three lowest OSL ages are within error of each other, and the combined age is 6.03 ± 0.48 ka.

Magnetic susceptibility

Magnetic susceptibility was used to complement OSL screening in identifying mineralogical changes within this section, a technique also used by Muñoz-Salinas *et al.* (2011). Magnetic susceptibility readings taken at approximately every 5 cm throughout the Cocklemill Burn section range from 0.242 to 4.810 × 10^{-3} SI units (Fig. 13). The sand units generally record the standard magnetic susceptibility values for dry or wet sand, which is between *c.* 0.3 and *c.* 1 × 10^{-3} SI units. The higher values in magnetic susceptibility correlate with gravel horizons within the section, with the occurrence of higher concentrations of ferromagnetic minerals, attributed to the presence of igneous pebbles and accessory minerals such as magnetite. The largest values occur in gravels at 1.21 and 7.21 m depth within the section (8.13 and 2.13 mOD, respectively). Within the sand units a step change in values was recorded around *c.* 4.3 to 4.7 m depth (*c.* 5.04–4.60 mOD), above which values in the sands generally return between 0.5–1 × 10^{-3} SI units (not including spikes at gravel horizons). Sands below 4.70 m depth that are recording values <0.5 × 10^{-3} SI units may identify a change in sediment deposition at this point.

Radiocarbon chronology

Two marine shells were radiocarbon dated, at 1.85 mOD from within the core, and in the uppermost shell horizon of

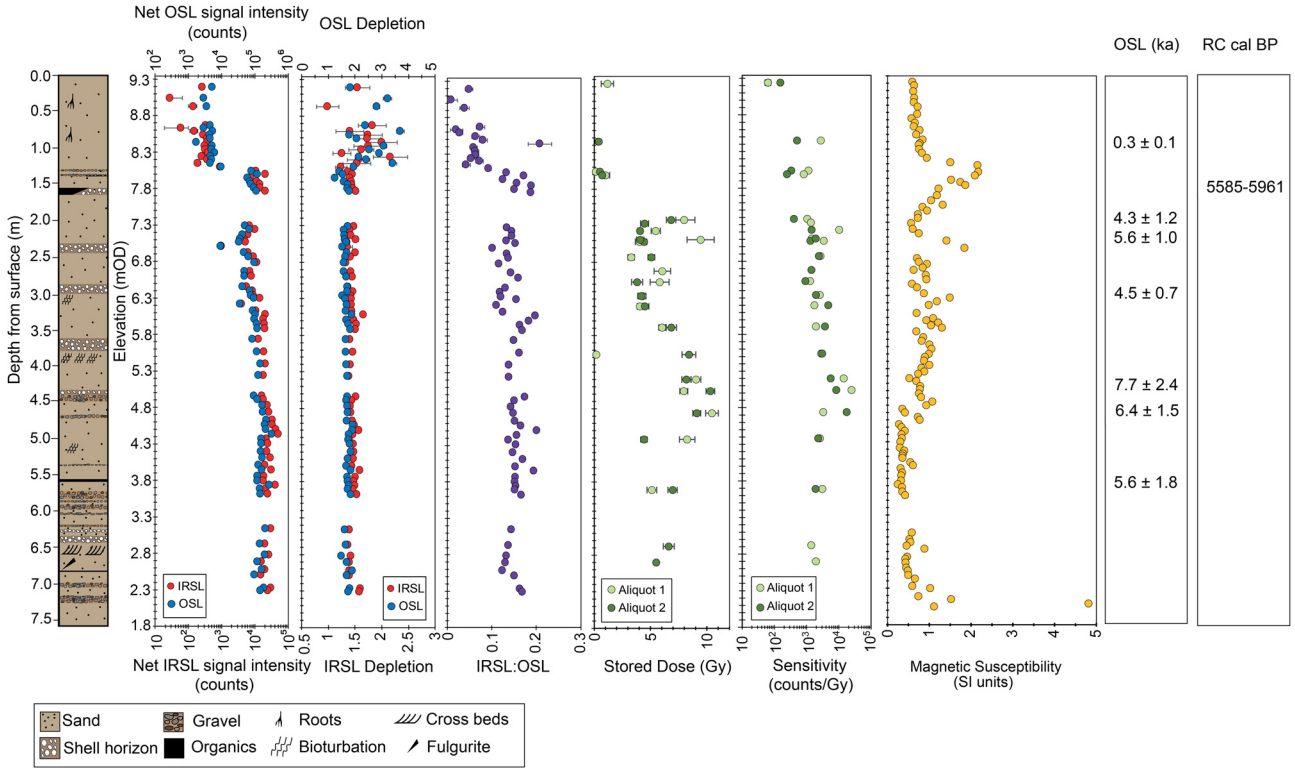

Fig. 13. Luminescence profiling, magnetic susceptibility readings and optically stimulated luminescence (OSL) (ka) and radiocarbon (RC) (cal years BP, 2σ error ranges) for Cocklemill Burn raised marine section (Locality 4).

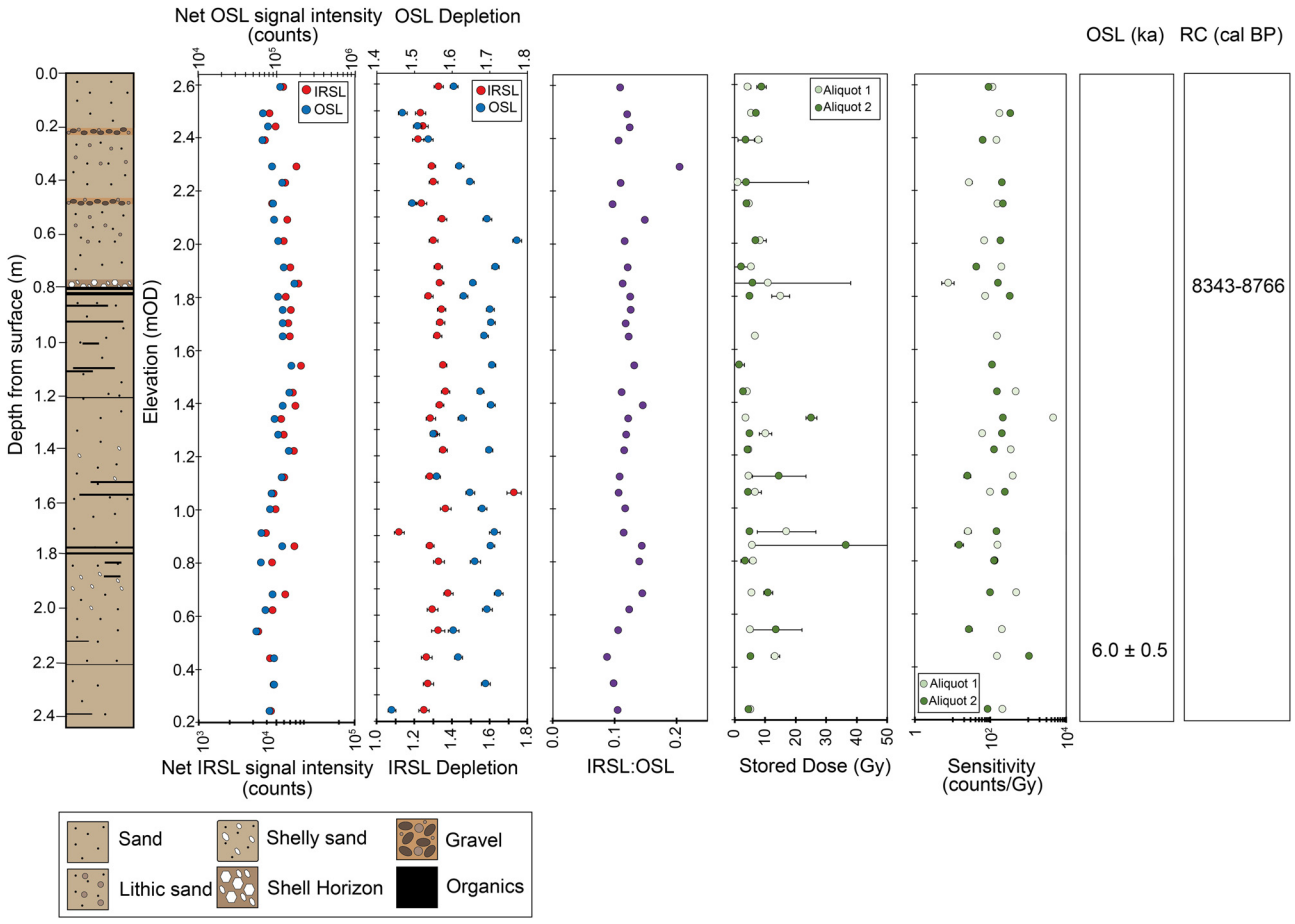

Fig. 14. Luminescence profiling and optically stimulated luminescence (OSL) (ka) and radiocarbon (RC) (cal years BP, 2σ error ranges) ages for the Cocklemill Burn core (Locality 4).

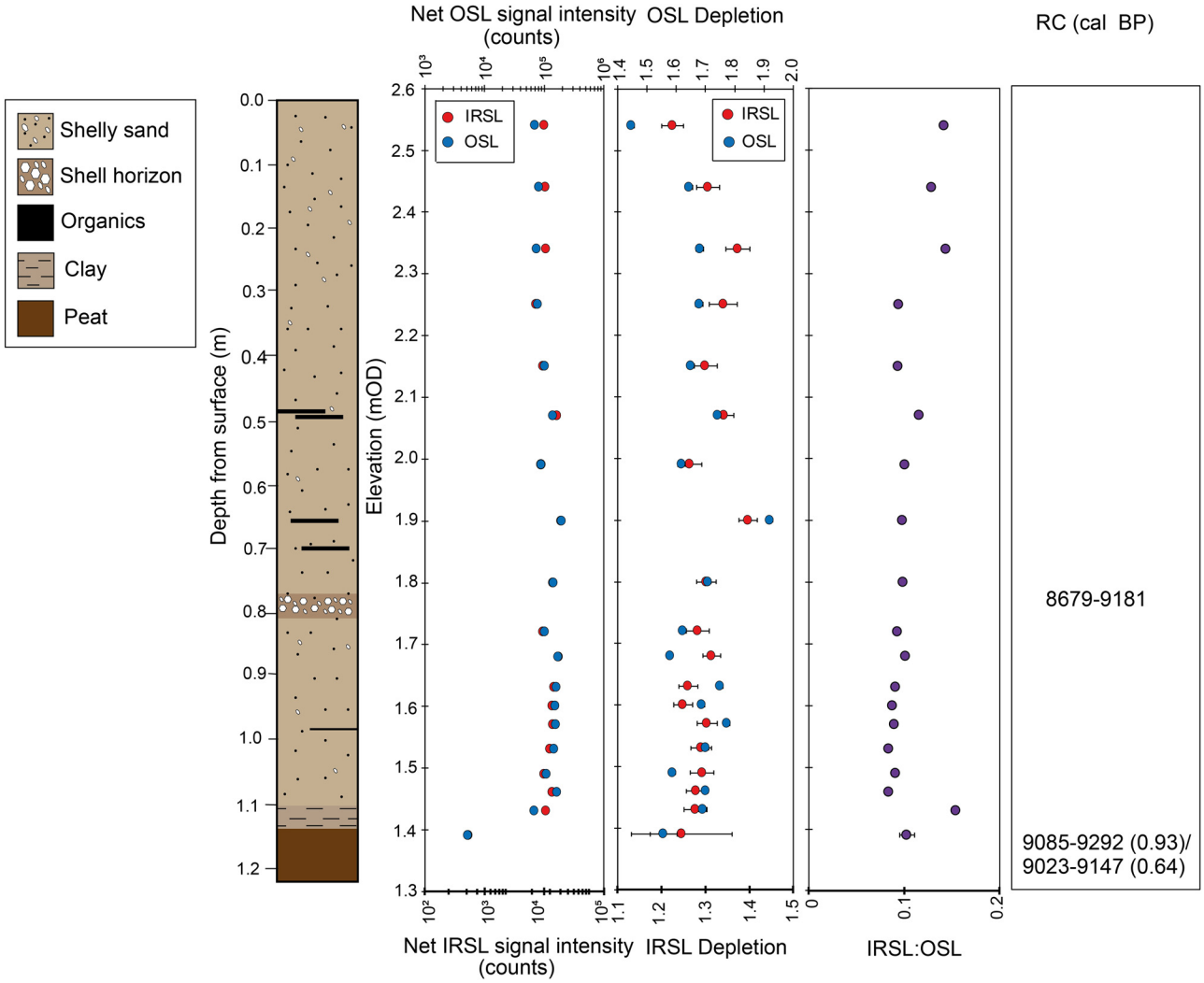

Fig. 15. Luminescence profiling and radiocarbon (RC) (cal years BP, 2σ error ranges) ages for Cocklemill Burn core (Locality 5).

the raised deposits at 7.78 mOD. The lower shell fragment was dated to 8343–8766 cal years BP, whilst the upper sample dated to 5585–5961 cal years BP. These radiocarbon samples sit within the luminescence profile for Cocklemill Burn; however, they are discordant with the OSL chronology, with both dates being older than the OSL ages stratigraphically below them. In the core at Locality 5 (Fig. 15), a shell fragment from the shell-rich layer (1.77 m OD) was radiocarbon dated to 8679–9181 cal years BP. This shell fragment is similar in age to the shell fragment dated in the core at Locality 4 at a similar elevation. Both humin and humic acid fractions of the basal peat sample collected were radiocarbon dated. The resulting dates fall within a part of the radiocarbon calibration curve with multiple potential results with corresponding probabilities in parentheses (Table 1). The humic acid fraction of the peat was dated with the highest probability to 9085–9292 cal years BP (93%) whilst the humin fraction of the peat was dated to 9023–9147 cal years BP (64%).

Discussion

Glacial sedimentation

The oldest dated sediments in the field area are the clays within the coastal (Locality 2) and saltmarsh (Locality 3) cores which yield ages in the range of *c.* 28–29 ka (CERSA446 and CERSA447 have a combined age of 28.25 ± 1.26 ka). These dates suggest that the clays were deposited during the last glacial period, with ice reaching this part of Fife prior to these dates. The glacial till exposed along the shoreface was most likely laid down by ice, and push structures on the till surface also hint at the role of significant glaciation during the deposition of the till. At the ice maximum over Scotland, thought to occur by 27 ka, the ice extended far to the east of the field site, joining with the Fennoscandian Ice Sheet (FIS) and therefore the ice at Ruddons Point may have persisted for some time after the age range of the dated sediments.

Previous nineteenth and early twentieth century accounts describe clays directly overlying till in the region (referred to as boulder-clay) and suggest that this clay was deposited in an Arctic climate. Brown (1867) describes an Arctic shell clay in the nearby area of Elie and likens it to that found at Errol, in the Tay Valley. Based on identification of shell species within the clay, the clay was interpreted to have been deposited in an Arctic cold climate when sea-level was around 150–200 ft (*c.* 45–60 m) higher than today. Brown (1867) goes on to postulate that the clay deposited directly above the boulder-clay at Elie could be largely contemporaneous with the development of the boulder-clay itself. This

observation would support the older dates of *c.* 28 and 29 ka, which were obtained from clays at the base of the coastal (Locality 2) and saltmarsh (Locality 3) cores. However, the clay at the base of each of these cores did not contain any obvious fossils or fossil fragments on observation, such as described by both Brown (1867) and Geikie (1902).

Timing of deglaciation in SE Scotland

The overlying lithic sands/sandy clay from the saltmarsh core dating to *c.* 18 ka at 0.08 mOD suggest these sediments were deposited much later than the pre-glacial clay below and point to deposition in the early post glacial landscape. There is still uncertainty as to the timing of initial deglaciation in the east of Scotland. Researchers who have focused on mapping the ice extent across the North Sea have suggested that the BIIS and the FIS were joined until 18.5 ka, with ice extending into the North Sea (Sejrup *et al.* 2016). Sissons *et al.* (1966) describe low-lying marine sediments at a similar elevation to those at Ruddons Point, which they map as underlying the carse clay, peat and high and main buried beaches in the Grangemouth area of the Inner Forth as Late Glacial in age; however, these sediments have not been dated. At a higher elevation along the Tay Valley, radiocarbon dates from +20 mOD raised clay deposits, known as the Errol Clay Formation, dated the ice retreat from the Wee Bankie Moraine and subsequent marine sedimentation to *c.* 14.5 ka BP (Peacock 2003). Raised marine silts at Lunan Bay recorded at *c.* +22 mOD have been dated earlier at 17 720 ± 50 years BP, suggesting that ice had already retreated westwards of this point at this time (McCabe *et al.* 2007). The BIIS is thought to have been highly dynamic in the North Sea Basin (Evans *et al.* 2021). The North Sea Lobe of the BIIS was fed by the Firth of Forth ice stream, which also had a strong influence on the retreat of the North Sea Lobe from 19.9–16.5 ka cal BP (Roberts *et al.* 2019). Dating of offshore glaciomarine sediments suggests that the deglaciation of the Forth had occurred by 16.9–16.0 ka cal BP (Roberts *et al.* 2019), with final retreat by 15.8 ka (Evans *et al.* 2021).

In this study, the environmental setting at *c.* 18.5 ka has been interpreted as a time of sea-level transgression, when the sea advanced inland due to the receding of the ice sheet westwards. During this time, modelled RSL curves from the Forth Valley suggest RSL was *c.* +40 m above present sea-level and the Tay Valley RSL curve suggests RSL would have been in excess of +25 m above present sea-level (Shennan *et al.* 2018, Fig. 1). Forsyth and Chisholm (1977) describe the Arctic clays at Elie as some of the oldest of the late glacial marine deposits and suggest they may have been disturbed by ice-push before the deposition of overlying sands. At St Monans, *c.* 7.5 km east of the Largo Bay field site, Geikie (1902, p. 310) describes sands and clays on the 100 ft terrace as being 'contorted', which suggests they have been overridden by ice. Geikie (1902) draws comparison between these clays of the 100 ft terrace at St Monans to the Arctic clays at Elie. This comparison could provide further evidence that these old ages from *c.* 18.5–29 ka, obtained from the Locality 2 and Locality 3 cores, show that sediment pre-dating the last glacial advance are preserved here. In this study, no evidence of glacio-tectonism was specifically noted within the cores themselves; however, potential ice-push structures were identified on the exposed clay surface close to the site of the coastal core (Fig. 8).

This study has not identified and dated sediments from the Late-glacial period, the period between 14.7 and 11.7 ka (Walker and Lowe 2019). However, previous researchers have suggested the higher (undated) raised rock platforms of the nearby Kincraig Point could have been formed during this time (e.g. Cullingford and Smith 1966), based on correlations to other shorelines in the region and the widely described '100 ft sea' marine incursion, which has long been documented across Fife (Geikie 1902; Rice 1961). However, these platforms could also represent older inherited features.

Buried peat and estuarine carseland sediments

The humin and humic acid radiocarbon dates, obtained from the peat horizon at Locality 5 (1.38 mOD), represent a period of lower relative sea-level at *c.* 9–9.3 ka. Sea-level remained below this elevation for a duration of time long enough to enable the formation of a terrestrial peat. The occurrence of a peat, directly underlying a grey/blue clay is reported at numerous locations in SE Scotland e.g. western Forth Valley (Sissons 1970) and at Flisk in north Fife (The SCAPE Trust 2021). The overlying fine, grey clay represents a relative sea-level rise, and return to estuarine conditions. This is known locally as the carse clay and marks the beginning of the Postglacial Marine Transgression (e.g. Smith *et al.* 1999).

The presence of a submerged forest at Largo Bay has also previously been suggested by Rev. Brown, who reported in the *New Statistical Account* the occurrence of a peat bed in Largo Bay, containing species of birch, hazel and alder as well as preserved trunks a number of feet in length (Gordon 1845). Based on the closest RSL model constructed for the Tay region by Shennan *et al.* (2018; Fig. 1), sea-level was *c.* 1 m above present-day sea-level at 9 ka; however, there is a spread of underlying data points at elevations ranging from *c.* +1 m to −5 m, showing the potential for significant variations in sea-level across the region.

Cocklemill Burn Holocene deposits

The raised deposits along the Cocklemill Burn record small-scale fluctuations in sea-level within an overall marine transgression, with the depositional environment staying in close proximity to the shore throughout. The presence of fragments of coal identified within the section reflect the location of the site in relation to the underlying bedrock geology of Carboniferous coal series.

Scenario 1: OSL chronology

OSL dating results in ages of *c.* 7.5–6 ka in the core and the lower part of the section. The samples in the upper marine sands were dated to *c.* 5.5–4.5 ka and, above this, the upper sand layers have been interpreted as windblown sands, with the uppermost sample dated to <300 years. Magnetic susceptibility results for the Cocklemill Burn section also point to a potential change in provenance or deposition history at *c.* 4.5 m depth in the section. This could mark a change in accumulation between the lower sediments of 7.5–6 ka, to a second accumulation of sands from 5.5–4.5 ka, as

sea-level was continuing to rise through the early to mid-Holocene. Smith *et al.* (2007) have described that much of the Scottish coastline falls within a convergence zone between the older identified Main Postglacial Shoreline and younger Blairdrummond shoreline, and therefore the two shorelines overlap one another.

Potential uranium mobility

Within the core at Locality 4, the OSL age of 6.02 ± 0.53 ka is younger than the radiocarbon date stratigraphically above it. The younger OSL age may be in part due to the proximity to the river and the sediments being waterlogged. A higher concentration of uranium may point to uranium solubility in the waterlogged sediments sampled within the core, with late deposition of uranium, resulting in an elevated environmental dose rate, and therefore a younger age (Olley *et al.* 1996). Assuming that the uranium concentrations would have originally been consistent with the ratio of Th: U in the sediments above, then the dose rate to this sample can be modelled. Assumed water content and effective dose rates for each dating sample are presented in Table 2 and radionuclide concentrations for each dosimetry sample are presented within the Supplementary material. Within the Cocklemill Burn section, the average ratio of Th: U is 3.19 (Fig. 16). Using this ratio to revise the estimate of uranium (ppm) in the CERSA473 dosimetry samples results in a modelled age of 6.26 ± 0.53 ka, bringing the age closer to concordance with the radiocarbon date stratigraphically above it, although a discrepancy between the two dating techniques is still apparent. With either estimate, the potential for the soluble radionuclides to be mobile suggests that this age needs to be interpreted as a minimum age. Using this modelled age, the new combined age of the lowest three OSL ages within this section (LL20, LL22 and CERSA473) is 6.23 ± 0.48 ka.

Scenario 2: radiocarbon chronology

The radiocarbon date from a shell fragment (1.77 mOD elevation) within the sands stratigraphically above the carse clay yielded an age of 9181–8679 cal years BP. A shell fragment collected at an elevation of 1.85 mOD from the core at Locality 4, dated to 8766–8343 cal years BP, therefore dates from both of the cores at Cocklemill Burn suggest that the high energy sands were being deposited on top of the carse clay in the early Holocene. The final radiocarbon date collected within the Cocklemill Burn section was selected from the uppermost sea-level horizon identified (7.78 mOD) and dated to 5961–5585 cal years BP. This radiocarbon age suggests that the raised marine deposits of Cocklemill Burn range from the early Holocene after the occurrence of the Postglacial Marine Transgression through to the mid-Holocene.

Previous studies at Cocklemill Burn

Previous studies along the Cocklemill Burn have yielded different age profiles (Fig. 17). In these studies, the OSL ages in general are younger than the radiocarbon ages at similar horizons. Previous OSL dating of the Cocklemill Burn sediments, obtained as part of an undergraduate dissertation by Overshott (2004; key results published in Dawson and Dawson 2007), interpreted the onset of postglacial marine

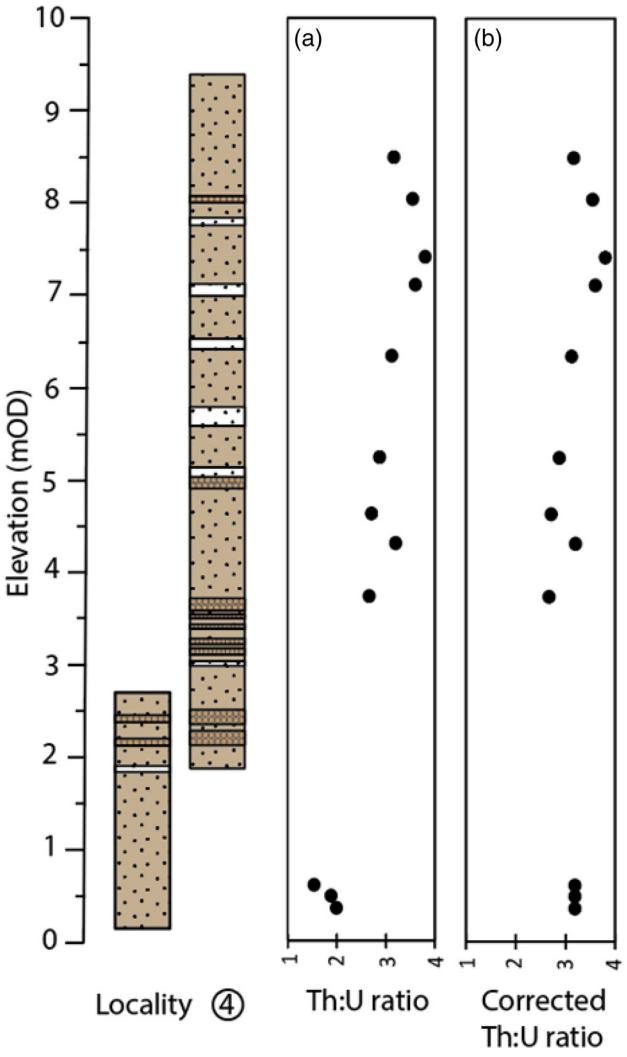

Fig. 16. (**a**) The Th: U ratio for each dosimetry sample within the Cocklemill Burn section and core (Locality 4) plotted against height in the section. (**b**) Th: U ratios for dosimetry samples CERSA473-A, -B and -C corrected to the average Th: U ratio through the overlying dosimetry samples.

transgression at 8130 ± 195 cal years BP, with transgression continuing until *c.* 6 ka. Two unconformities were identified within the stratigraphy, the first at 6 ka and the second between 4.5 and 2.5 ka. The stratigraphically highest date obtained within the Overshott (2004) study was 2.58 ± 0.10 ka, which is younger than the dates identified by Tooley and Smith (2005) or in this current study at a similar elevation; however, the Cocklemill Burn section studied within the current study was situated *c.* 80 m further inland.

Tooley and Smith (2005) report five radiocarbon dates through the raised marine deposits exposed along the Cocklemill Burn. They conclude that the marine sediments range in age from 9000 to 5280 cal years BP (as calibrated in 2005) and represent the two raised shorelines of the Main Postglacial Shoreline and Blairdrummond Shoreline. They also equate the high-energy gravels at the base of the Cocklemill section to the Storegga Slide event (2.26–4.03 mOD), which is recorded at numerous field sites around the Scottish coastline, although usually as a sand layer within estuarine clays. The tsunami event has recently been dated within the Montrose Basin, Angus, using OSL to 8.10 ± 0.25 ka (Bateman *et al.* 2021). Tooley and Smith

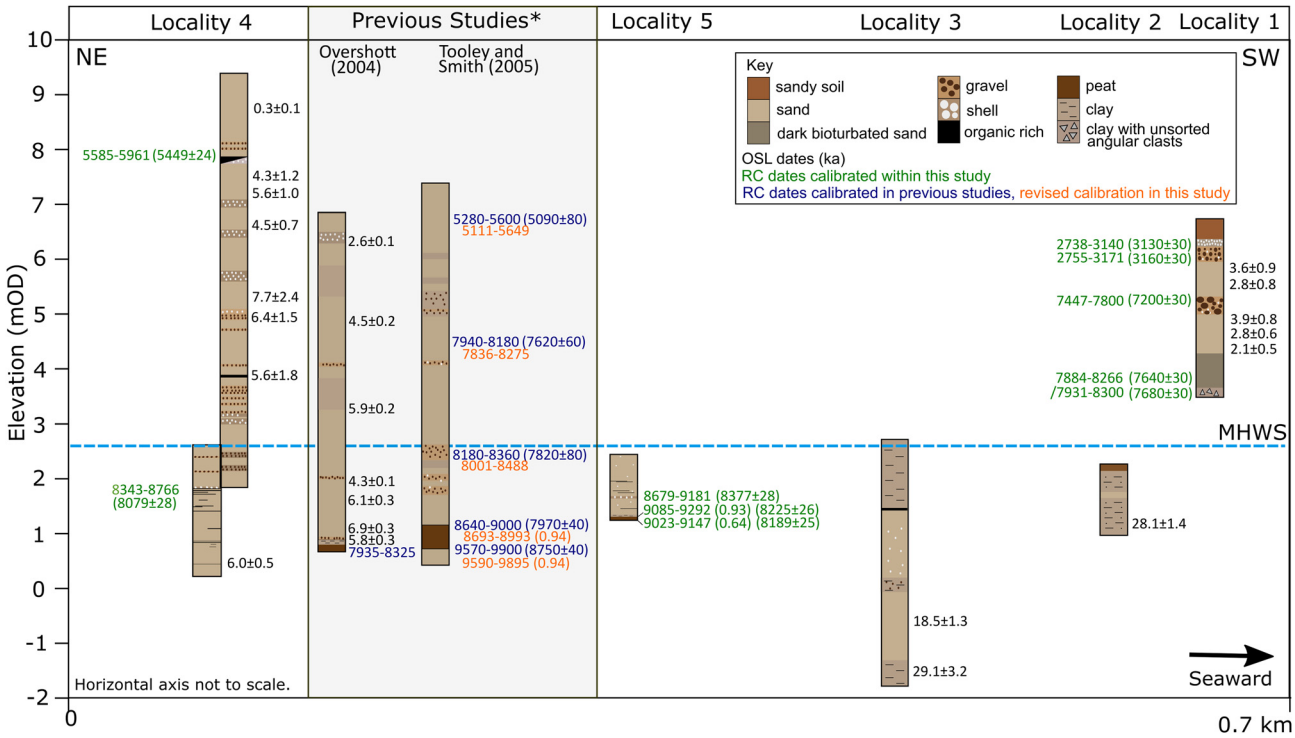

Fig. 17. Simplification of raised deposits and cores collected in this study across all five field localities of Largo Bay. Two summarized illustrations of previous studies at Cocklemill Burn are also presented to compare dated sections to the current study (results from Overshott (2004), as published in Dawson and Dawson (2007), and Tooley and Smith (2005). Radiocarbon dates are presented as calibrated ages (cal years BP) followed by the uncalibrated radiocarbon age in parentheses.

(2005) dated a marine shell between 2.49 and 2.44 mOD within the Cocklemill raised marine deposits to 8180–8360 cal years BP (calibrated in 2005) which they describe as redeposited and therefore the Storegga event occurred after this time. Overshott (2004) discusses the possibility of a thin clast and sand horizon, located directly above the carse clay at *c.* 0.8 mOD, of being related to the Storegga event; however, the corresponding OSL age obtained at this elevation is younger at 6.86 ± 0.3 ka (dates published in Dawson and Dawson 2007). OSL dates from both the Overshott (2004) and the current study would place the sand and gravel deposits in the section as younger than the Storegga event. Within the current study, the lowest OSL age from the sands of the Cocklemill core is also younger than the age of the Storegga event; however, this could be underestimated due to the proximity to the Cocklemill Burn river and the associated effect on the environmental dose. If this lowest OSL age is discounted, and instead only the radiocarbon age at 1.85 mOD of 8343–8766 cal years BP is considered, then the high-energy gravel deposits at the base of the section, which are stratigraphically above this dated horizon, could have been deposited within the age range of the Storegga Slide tsunami event. The high-energy gravel deposits have not been directly dated within this study.

Ruddons Point Holocene deposits

Short OSL chronology

OSL dating of the raised marine deposits at Ruddons Point yields ages in the range of *c.* 2.0–3.9 ka. The darker, organic-rich sands at the base of the section above the till were not dated through OSL, due to the low luminescence signal noted during initial screening using the portable OSL reader. All of the Ruddons Point OSL samples display high σd of *c.* 30–50%. High rates of σd can be due to multiple reasons such as sediment mixing through processes such as bioturbation, incomplete bleaching at the point of deposition and variable environmental dosimetry (Galbraith and Roberts 2012). At Ruddons Point, the presence of modern roots through the section could have contributed to sediment mixing, and the high-energy nature of the deposition of the gravels could have mixed older incompletely bleached sediments with sediments bleached upon deposition. The presence of the two gravel units and smaller gravel clasts through the sands could also suggest small changes in environmental dosimetry, all of which could be contributing to a high σd. Complementary microfossil analysis conducted at Ruddons Point picked out a distinct environmental change between the darker inhospitable sands at the base of the section and the more hospitable sands above.

RSLs are thought to have been falling during this time and this is potentially why these younger deposits are constrained further seaward, potentially onlapping older sediments at the same elevation, and not noted at the Cocklemill Burn location further inland. Modelled RSL curves for the Forth and Tay regions (e.g. Shennan *et al.* 2018, Fig. 1) show a gradual fall in RSL over the late Holocene; however, the formation of the Ruddons Point raised deposits may suggest a more punctuated change in sea-level to allow the formation of this shoreline. The difference between the smoothed GIA models and the empirical evidence is also noted further inland along the Firth of Forth by Smith *et al.* (2010) who describe a shoreline with a mean radiocarbon age of 3600 years BP. This is of similar age to the upper Ruddons Point sediments; however, the different uplift rates between the inner Forth sites, closer to the uplift centre and the field

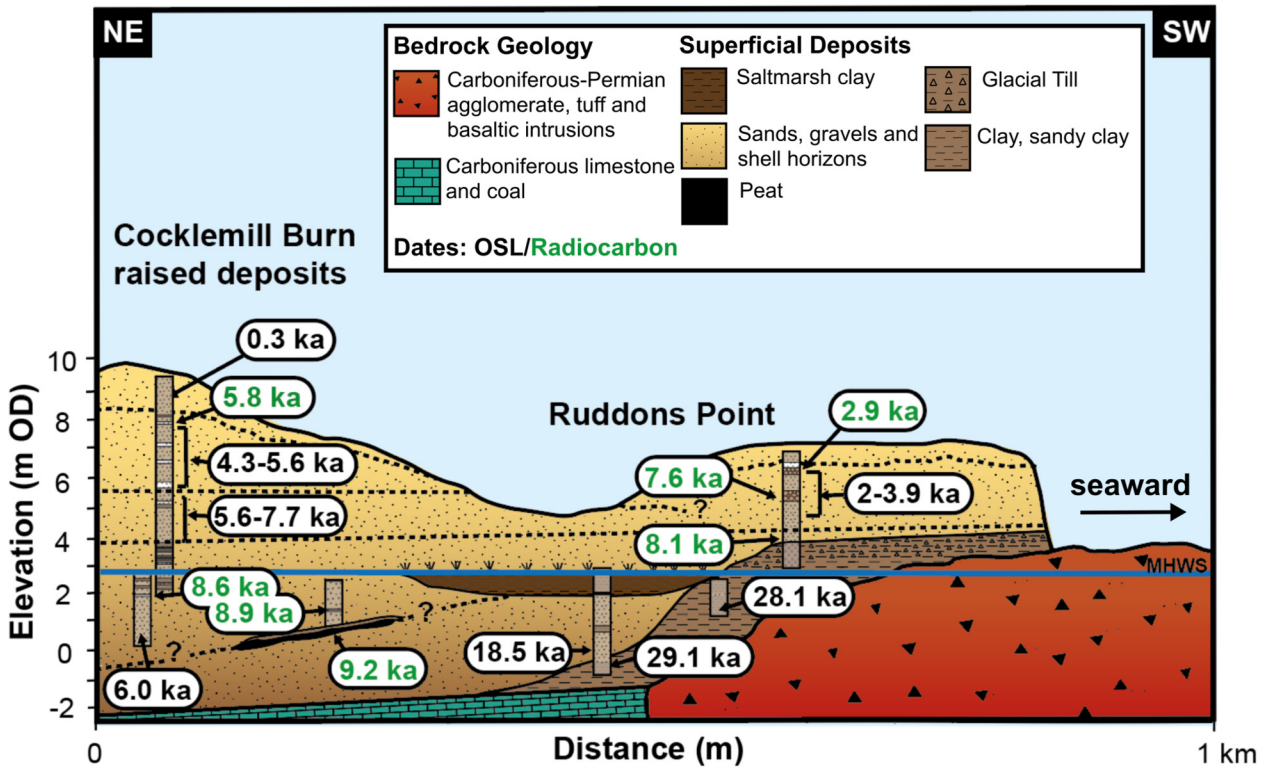

Fig. 18. Schematic illustration of raised marine deposits and cores collected in this study across all five field localities of Largo Bay. Radiocarbon ages in green; optically stimulated luminescence (OSL) dates in black. Radiocarbon dates are presented in calibrated years BP (cal years BP) to be more closely comparable to the OSL dates, which are relative to the year 2019/20.

site at Ruddons Point, *c.* 60 km further east, make it difficult to correlate.

Long OSL and radiocarbon chronology

The radiocarbon sampling focused on dating marine shell and shell fragments and provides an extended chronology beyond the sand units dated through OSL. The shell fragments from the base of the section were dated to 7884–8266 cal years BP and 7931–8300 cal years BP. The timing of the Storegga Slide event falls within the age range of these dated shells; however, further detailed investigation into confirming the presence of tsunamiite deposits at Ruddons Point was not carried out within this study. Within the lower gravel/cobble unit, the dated marine shell yielded an age of 7447–7899 cal years BP, suggesting that there is an age difference of *c.* 4.6 ka between this gravel unit and the upper gravel which was dated to between 2738 and 3171 cal years BP. These results suggest that the Ruddons Point raised marine deposits record deposition from the end of the early Holocene right through to the late Holocene, whereas dating of only the sand units through OSL yielded ages of the late Holocene only. A summary schematic of the field site is shown in Figure 18.

Conclusions

This study delivers a detailed study of the complex environmental changes that have occurred in the SE of Scotland as a result of eustatic sea-level changes and crustal responses to the last deglaciation of Scotland. Results from this study include:

(1) Undertaking an initial geophysical survey that identified buried features and aided in interpreting the characteristics of underlying sediments, which could be related to subsequent coring.
(2) The utilization of portable OSL equipment to create high-resolution luminescence stratigraphies for raised marine deposits and subsurface sediments cored at Largo Bay, which allowed hypotheses concerning depositional sequences to be generated in near real-time and guided sample positing for dating. The OSL chronology for the depositional sequences was augmented, and expanded, by the collection of shells from the raised marine deposits as well as sampling humin and humic fractions from the buried peats for radiocarbon dating. The comparison of two dating methods allowed for a critical assessment of results and the development of different depositional scenarios.
(3) Building a chronology of the coastal and saltmarsh cores (Localities 1 and 2) spanning from the onset of the LGM, to the post-glacial marine sediments dated to *c.* 18 ka was obtained through OSL dating.
(4) Radiocarbon dating the basal peat at Locality 5 using both humin and humic acid fractions to the early Holocene at *c.* 9.2 ka. This was a period of relative sea-level fall when the sea-level was lower than present day, allowing the terrestrial peat to form. The peats are overlain by carse clay, which represents the beginning of the Postglacial Marine Transgression and a subsequent period of relative sea-level rise.

(5) Dating of the inland raised marine sand and gravel deposits records small-scale fluctuations in sea-level in the early to mid-Holocene, capped with much younger <300-year-old windblown sands. The Cocklemill section contains sediments of Blairdrummond Shoreline age overlapping Main Postglacial Shoreline age sediments. OSL dating suggested sediments within the section and core were younger than that of the Storegga Slide tsunami; however, radiocarbon dates at both the Cocklemill and Ruddons Point sections suggest that the sediments do encompass this time period, as concluded in the previous study by Tooley and Smith (2005).
(6) Magnetic susceptibility measurements were employed and used to interpret depositional changes within the raised marine deposits.
(7) OSL dating of the Ruddons Point raised marine sand and gravel indicates that they were deposited in the late Holocene; however, high σd values of 30–50% and evidence of age inversions within the section suggests high-energy deposition with significant mixing and reworking of sediments.
(8) Microfossil analysis of the sediments of Ruddons Point identified an inhospitable organic-rich environment at the base of the section and a hospitable environment in the sediments above. The upper sand is much less fossiliferous which suggests a different depositional setting to the sediments below.

The field area provided an opportunity to examine the changing environment and depositional history through both the Late Devensian and Holocene. The multidisciplinary investigation has demonstrated the value of detailed local-scale field study to evaluate and gain a fuller understanding of past sea-level change. This method can be utilized in future coastal change studies in Scotland or in similar coastal environments worldwide where fewer studies have been conducted or detailed RSL information is missing as the comparison of dating methods builds a fuller appreciation for complex RSL variations and coastal evolution.

Acknowledgements Thanks to Abbeyford Holiday Park and Scottish Natural Heritage for permission to undertake field studies and sample at the site. Thanks to Tim Raub for his supervision of this PhD project and assistance with sample collection, and also to Martin Bates, Tony Prave and Noel Lasway for assistance in the field. Thanks to Ruth Robinson for providing details of previous unpublished OSL data from the field site and to Andrea Burke for funding additional radiocarbon analyses. Thanks to the two reviewers for their constructive feedback on the manuscript.

Author contributions **SLB**: formal analysis (lead), investigation (lead), methodology (lead), project administration (lead), visualization (lead), writing – original draft (lead), writing – review & editing (lead); **TCK**: formal analysis (supporting), investigation (supporting), methodology (supporting), resources (lead), supervision (equal), writing – review & editing (supporting); **AS**: formal analysis (supporting), writing – review & editing (supporting); **JEW**: formal analysis (supporting); **CRB**: conceptualization (equal), formal analysis (supporting), investigation (supporting), methodology (supporting), supervision (equal), writing – review & editing (supporting)

Funding This work was supported as part of SLB's PhD funding from The School of Earth and Environmental Sciences, The University of St Andrews, with additional funding from the SEES Small Research Grant.

Competing interests The authors declare that they have no known competing financial interests or personal relationships that could have appeared to influence the work reported in this paper.

Data availability All data generated or analysed during this study are included in this published article (and its supplementary information files).

Scientific editing by Martin Kirkbride

References

Ballantyne, C.K. and Small, D. 2018. The last Scottish ice sheet. *Earth and Environmental Science Transactions of the Royal Society of Edinburgh*, **110**, 93–131, https://doi.org/10.1017/S1755691018000038

Ballantyne, C.K., Hall, A.M. and Dawson, A.G. 2021. The Quaternary in Scotland. *In*: Ballantyne, C.K. and Gordon, J.E. (eds) *Landscapes and Landforms of Scotland*, 1st edn. Springer, 53–96, https://doi.org/10.1007/978-3-030-71246-4

Bateman, M.D., Kinnaird, T.C., Hill, J., Ashurst, R.A., Mohan, J., Bateman, R.B.I. and Robinson, R. 2021. Detailing the impact of the Storegga Tsunami at Montrose, Scotland. *Boreas*, **50**, 1059–1078, https://doi.org/10.1111/bor.12532

Bickerdike, H.L., Evans, D.J.A., ÓCofaigh, C. and Stokes, C.R. 2016. The glacial geomorphology of the Loch Lomond Stadial in Britain: a map and geographic information system resource of published evidence. *Journal of Maps*, **12**, 1178–1186, https://doi.org/10.1080/17445647.2016.1145149

Bradley, S.L., Milne, G.A., Shennan, I. and Edwards, R. 2011. An improved glacial isostatic adjustment model for the British Isles. *Journal of Quaternary Science*, **26**, 541–552, https://doi.org/10.1002/jqs.1481

Brown, T. 1867. On the arctic shell-clay of Elie and Errol. *Transactions of the Royal Society of Edinburgh*, **24**, 617–633, https://doi.org/10.1017/S0080456800020500

Chapman, N.A. 1976. Inclusions and megacrysts from undersaturated tuffs and basanites, East Fife, Scotland. *Journal of Petrology*, **17**, 472–498, https://doi.org/10.1093/petrology/17.4.472

Chiverrell, R.C. and Thomas, G.S.P. 2010. Extent and timing of the Last Glacial Maximum (LGM) in Britain and Ireland: a review. *Journal of Quaternary Science*, **25**, 535–549, https://doi.org/10.1002/jqs.1404

Costa, P.J.M., Dawson, S., Ramalho, R.S., Engel, M., Dourado, F., Bosnic, I. and Andrade, C. 2021. A review on onshore tsunami deposits along the Atlantic coasts. *Earth-Science Reviews*, **212**, 103441, https://doi.org/10.1016/j.earscirev.2020.103441

Cullingford, R.A. and Smith, D.E. 1966. Late-glacial shorelines in Eastern Fife. *Transactions of the Institute of British Geographers*, **39**, 31–51, https://doi.org/10.2307/621673

Dawson, A.G., Long, D. and Smith, D.E. 1988. The Storegga Slides: Evidence from eastern Scotland for a possible tsunami. *Marine Geology*, **82**, 271–276, https://doi.org/10.1016/0025-3227(88)90146-6

Dawson, S. and Dawson, A. 2007. Field Guide: IGCP 495 (UK Working Group) and INQUA Coastal and Marine Processes (NW Europe Working Group), St Andrews, 1–4 July 2007.

Dietze, M., Kreutzer, S., Burow, C., Fuchs, M.C., Fischer, M. and Schmidt, C. 2016. The abanico plot: visualising chronometric data with individual standard errors. *Quaternary Geochronology*, **31**, 12–18, https://doi.org/10.1016/j.quageo.2015.09.003

Evans, D.J.A., Roberts, D.H., Bateman, M.D. *et al.*. 2021. Retreat dynamics of the eastern sector of the British Irish Ice Sheet during the last glaciation. *Journal of Quaternary Science*, **36**, 723–751, https://doi.org/10.1002/jqs.3275

Forsyth, I.H. and Chisholm, J.I. 1977. *The Geology of East Fife*. Her Majesty's Stationery Office, Edinburgh.

Galbraith, R.F. and Roberts, R.G. 2012. Statistical aspects of equivalent dose and error calculation and display in OSL dating: an overview and some recommendations. *Quaternary Geochronology*, **11**, 1–27, https://doi.org/10.1016/j.quageo.2012.04.020

Galbraith, R.F., Roberts, R.G., Laslett, G.M., Yoshida, H. and Olley, J.M. 1999. Optical dating of single and multiple grains of quartz from Jinmium rock shelter, northern Australia: Part I, experimental design and statistical models. *Archaeometry*, **41**, 339–364, https://doi.org/10.1111/j.1475-4754.1999.tb00987.x

Geikie, A. 1902. *The Geology of Eastern Fife*. Her Majesty's Stationery Office, Glasgow.

Gordon, J. (ed.) 1845. *The New Statistical Account of Scotland/by the ministers of the Respective Parishes, Under the Superintendence of a Committee of the Society for the Benefit of the Sons and Daughters of the Clergy. Largo, Fife*. Blackwoods and Sons, Edinburgh, **9**, 434, https://stataccscot.edina.ac.uk:443/link/nsa-vol19-p434-parish-fife-largo

Hamilton, W.J. 1835. Description of a bed of recent marine shells near Elie, on the southern coast of Fifeshire. *Proceedings of the Geological Association of London*, **2**, 180–181.

Harkness, D.D. 1983. The extent of natural 14C deficiency in the coastal environment of the United Kingdom. *Journal of the European Study Group on Physical, Chemical and Mathematical Techniques Applied to Archaeology PACT*, **8**, 351–364.

Heaton, T.J., Köhler, P. *et al.*. 2020. Marine20 – The marine radiocarbon age calibration curve (0–55 000 cal BP). *Radiocarbon*, **62**, 779–820, https://doi.org/10.1017/RDC.2020.68

Jardine, W.G. 1982. Sea-level changes in Scotland during the last 18 000 years. *Proceedings of the Geologists' Association*, **93**, 25–41, https://doi.org/10.1016/S0016-7878(82)80030-8

Kim, J., Løvholt, F., Issler, D. and Forsberg, C.F. 2019. Landslide material control on tsunami genesis – the Storegga Slide and tsunami (8100 years BP). *Journal of Geophysical Research: Oceans*, **124**, 3607–3627, https://doi.org/10.1029/2018JC014893

Kinnaird, T., Bolòs, J., Turner, A. and Turner, S. 2017. Optically-stimulated luminescence profiling and dating of historic agricultural terraces in Catalonia (Spain). *Journal of Archaeological Science*, **78**, 66–77, https://doi.org/10.1016/j.jas.2016.11.003

Kuchar, J., Milne, G., Hubbard, A., Patton, H., Bradley, S., Shennan, I. and Edwards, R. 2012. Evaluation of a numerical model of the British–Irish ice sheet using relative sea-level data: implications for the interpretation of trimline observations. *Journal of Quaternary Science*, **27**, 597–605, https://doi.org/10.1002/jqs.2552

McCabe, A.M., Clark, P.U., Smith, D.E. and Dunlop, P. 2007. A revised model for the last deglaciation of eastern Scotland. *Journal of the Geological Society, London*, **164**, 313–316, https://doi.org/10.1144/0016-76492006-120

Mejdahl, V. 1979. Thermoluminescence dating: Beta-dose attenuation in quartz grains. *Archeometry*, **29**, 61–72, https://doi.org/10.1111/j.1475-4754.1979.tb00241.x

Merritt, J.W., Hall, A.M., Gordon, J.E. and Connell, E.R. 2019. Late Pleistocene sediments, landform and events in Scotland: a review of the terrestrial stratigraphic record. *Earth and Environmental Science Transactions of the Royal Society of Edinburgh*, **110**, 39–91, https://doi.org/10.1017/S1755691018000890

Milne, G.A., Shennan, I. *et al.* 2006. Modelling the glacial isostatic adjustment of the UK region. *Philosophical Transactions of the Royal Society*, **364**, 931–948, https://doi.org/10.1098/rsta.2006.1747

Muñoz-Salinas, E., Bishop, P., Sanderson, D.C.W. and Zamorano, J.-J. 2011. Interpreting luminescence data from a portable OSL reader: three case studies in fluvial settings. *Earth Surface Processes and Landforms*, **36**, 651–660, https://doi.org/10.1002/esp.2084

Munyikwa, K., Kinnaird, T.C. and Sanderson, D.C.W. 2021. The potential of portable luminescence readers in geomorphological investigations: a review. *Earth Surface Processes and Landforms*, **46**, 131–150, https://doi.org/10.1002/esp.4975

Murray, A.S. and Wintle, A.G. 2000. Luminescence dating of quartz using an improved single-aliquot regenerative-dose protocol. *Radiation Measurements*, **32**, 57–73, https://doi.org/10.1016/S1350-4487(99)00253-X

Murray, J.W. 2006. *Ecology and Applications of Benthic Foraminifera*. Cambridge University Press.

Olley, J.M., Murray, A. and Roberts, R. 1996. The effects of disequilbria in the Uranium and Thorium decay chains on burial dose rates in fluvial sediments. *Quaternary Science Reviews*, **15**, 751–760, https://doi.org/10.1016/0277-3791(96)00026-1

Overshott, K.E. 2004. *Optical Stimulated Luminescence (OSL) and Holocene dune sands in Largo Bay*. Undergraduate dissertation, Department of Geography and Geosciences, University of St Andrews.

Peacock, J.D. 2003. Late Devensian marine deposits (Errol Clay Formation) at the Gallowflat Claypit, eastern Scotland: new evidence for the timing of ice recession in the Tay estuary. *Scottish Journal of Geology*, **39**, 1–10, https://doi.org/10.1144/sjg39010001

Reimer, P.J., Austin, W.E.N. *et al.*. 2020. The IntCal20 Northern Hemisphere radiocarbon age calibration curve (0–55 cal kBP). *Radiocarbon*, **62**, 725–757, https://doi.org/10.1017/RDC.2020.41

Rennie, A.F. and Hansom, J.D. 2011. Sea level trend reversal: land uplift outpaced by sea level rise on Scotland's coast. *Geomorphology*, **125**, 193–202, https://doi.org/10.1016/j.geomorph.2010.09.015

Rice, R.J. 1961. The glacial deposits at St. Fort in north-eastern Fife: a re-examination. *Transactions of the Edinburgh Geological Society*, **18**, 113–123, https://doi.org/10.1144/transed.18.2.113

Roberts, D.H., Evans, D.J.A. *et al.* 2018. Ice marginal dynamics of the last British–Irish Ice Sheet in the southern North Sea: ice limits, timing and the influence of the Dogger Bank. *Quaternary Science Reviews*, **198**, 181–207, https://doi.org/10.1016/j.quascirev.2018.08.010

Roberts, D.H., Grimoldi, E. *et al.* 2019. The mixed-bed glacial landform imprint of the North Sea Lobe in the western North Sea. *Earth Surface Processes and Landforms*, **44**, 1233–1258, https://doi.org/10.1002/esp.4569

Sejrup, H.P., Clark, C.D. and Hjelstuen, B.O. 2016. Rapid ice sheet retreat triggered by ice stream debuttressing: evidence from the North Sea. *Geology*, **44**, 355–358, https://doi.org/10.1130/G37652.1

Shennan, I., Bradley, S.L. and Edwards, R. 2018. Relative sea-level changes and crustal movements in Britain and Ireland since the Last Glacial Maximum. *Quaternary Science Reviews*, **188**, 143–159, https://doi.org/10.1016/j.quascirev.2018.03.031

Sissons, J.B. 1967. *The Evolution of Scotland's Scenery*. Oliver and Boyd Ltd, Edinburgh.

Sissons, J.B. 1970. Dislocation and non-uniform uplift of raised shorelines in the western part of the Forth valley. *Transactions of the Institute of British Geographers*, **55**, 145–159, https://doi.org/10.2307/621727

Sissons, J.B. 1974. The Quaternary in Scotland: a review. *Scottish Journal of Geology*, **10**, 311–337, https://doi.org/10.1144/sjg10040311

Sissons, J.B., Smith, D.E. and Cullingford, R.A. 1966. Late-glacial and post-glacial shorelines in south-east Scotland. *Transactions of the Institute of British Geographers*, **39**, 9–18, https://doi.org/10.2307/621671

Smith, D.E., Sissons, J.B. and Cullingford, R.A. 1969. Isobases for the Main Perth Raised Shoreline in South-East Scotland as determined by trend-surface analysis. *Transactions of the Institute of British Geographers*, **46**, 45–52, https://doi.org/10.2307/621407

Smith, D.E., Firth, C.R., Brooks, C.L., Robinson, M. and Collins, P.E.F. 1999. Relative sea-level rise during the Main Postglacial Transgression in NE Scotland, UK. *Transactions of the Royal Society of Edinburgh: Earth Sciences*, **90**, 1–27, https://doi.org/10.1017/S0263593300002480

Smith, D.E., Firth, C.R. and Cullingford, R.A. 2002. Relative sea-level trends during the early-middle Holocene along the eastern coast of mainland Scotland, UK. *Boreas*, **31**, 185–202, https://doi.org/10.1111/j.1502-3885.2002.tb01065.x

Smith, D.E., Cullingford, R.A., Mighall, T.M., Jordan, J.T. and Fretwell, P.T. 2007. Holocene relative sea level changes in a glacio-isostatic area: new data from south-west Scotland, United Kingdom. *Marine Geology*, **242**, 5–36, https://doi.org/10.1016/j.margeo.2006.09.015

Smith, D.E., Davies, M.H. *et al.* 2010. Holocene relative sea levels and related prehistoric activity in the Forth lowland, Scotland, United Kingdom. *Quaternary Science Reviews*, **29**, 2382–2410, https://doi.org/10.1016/j.quascirev.2010.06.003

Smith, D.E., Barlow, N.L.M., Bradley, S.L., Firth, C.R., Hall, A.M., Jordan, J.T. and Long, D. 2019. Quaternary sea level change in Scotland. *Earth and Environmental Science Transactions of the Royal Society of Edinburgh*, **110**, 219–256, https://doi.org/10.1017/S1755691017000469

Stuiver, M. and Reimer, P.J. 1993. Extended 14C data base and revised CALIB 3.0 14C age calibration program. *Radiocarbon*, **35**, 215–230, https://doi.org/10.1017/S0033822200013904

Stuiver, M., Reimer, P.J. and Reimer, R.W. 2021. CALIB 8.2 [WWW program] at http://calib.org [last accessed 19 January 2021].

The National Oceanography Centre 2021. *Leith tide gauge site*, https://www.ntslf.org/tgi/portinfo?port=Leith [last accessed 11 February 2021].

The SCAPE Trust 2021. Flisk Seabraes submerged forest (1811), https://scapetrust.org/sites-at-risk/site/1811/ [last accessed 21 June 2021].

Tooley, M.J. and Smith, D.E. 2005. Relative sea-level change and evidence for the Holocene Storegga Slide tsunami from a high-energy coastal environment: Cocklemill Burn, Fife, Scotland, UK. *Quaternary International*, **133–134**, 107–119, https://doi.org/10.1016/j.quaint.2004.10.007

Walker, M. and Lowe, J. 2019. Lateglacial environmental change in Scotland. *Earth and Environmental Science Transactions of the Royal Society of Edinburgh*, **110**, 173–198, https://doi.org/10.1017/S1755691017000184